Ministry of Higher Education
& Scientific Research
AL-Muthanna University
College of Science
Chemistry Department

Hydrothermal Synthesis of ZnO / CdS Nano Composite as a Photo catalyst for removing of Textile dyes

A thesis submitted to the Chemistry Department / College of Science Al-Muthanna University in partial fulfillment of the requirement for the Master degree in Chemistry Science

By

Methal Naeem Mohwes

B. Sc. 2015

Supervised By

Professor
Dr.Ayad Fadhil Mohmmed

Assistant Professor
Dr. Khawla Kani Jassim

2023 A.D 1444 A.H

Certification of The Supervisor

I certify that this thesis entitled '' **Hydrothermal Synthesis of ZnO / CdS Nano Composite as a Photo catalyst for removing of Textile dyes**'' was done by '' **Methal Naeem Mohwes** '' under my supervision in the Department of Chemistry/College of Science/ Al-Muthanna University, in partial fulfillment of the requirements for the Master's degree in Chemistry.

Professor

Dr. Ayad Fadhil Alkaim

University of Babylon

College of Science

/ / 2023

Assistant Professor

Dr. Khawla Kani Jassim

Al-Muthanna University

College of Sciences

/ / 2023

In view of the available recommendations, I forward this thesis for debate by the examining committee.

Assist. Prof

Dr. Khawla Kani Jassim

Head of Department of Chemistry

Data: / /2023

Dedication...

To those who give up their ease and joy in sacrifice for the development of their kid .I am dedicating this letter to all working mothers

To whom I wish was with me... my father, who passed away

To the one who taught me manners, the source of tenderness... my dear mother

To the incorporeal motivation and the center of optimism, without him I would not have completed my career... my husband

My support in life... my brothers and sisters

All my loyal friends, and everyone who gave me a hand of help or a love

Methal Naeem

Acknowledgements

In the name of Allah, the most Merciful and most Gracious. First of all, I thank Allah, for inspiring me with strength, patience and willingness to perform this research.

I wish to express my deepest gratitude to my supervisors **Prof. Dr. Ayad Fadhil Alkaim and Assist. Prof. Dr. Khawla Kani Jasim** for introducing me to the interesting field of science and for providing me with the opportunity to carry out this study. I also thank them for invaluable advice, patience and inspiring guidance throughout this work.

I am also most grateful to **Dr. Aseel Aljeboree** For her support and great kindness towards me I would like to thank all the staff of the University of Babylon / College of Science for Women Laboratory Nanotechnology for their serious cooperation with me, I am sincerely indebted and grateful to everyone who helped me in this work.

My special thanks to both (Inaam Gouda and Ahmed Mashhour) for their help and their beautiful and unforgettable situations.

I would like to thank all staff members of the Department of Chemistry a, The College of Science at Al-Muthanna University, for their valuable help and advice.

I am extremely grateful to my parents for their love, prayers, caring, and sacrifices for educating and preparing me for my future. I am very thankful to my dear Husband for his love, and understanding, also I am very Grateful to my dear sisters and brothers for their love, understanding prayers, and continuing support to completing this research work.

Methal Naeem

بِسْمِ اللهِ الرَّحْمٰنِ الرَّحِيم

ۣ

﴿إِنَّ الَّذِينَ آمَنُوا وَعَمِلُوا الصَّالِحَاتِ يَهْدِيهِمْ رَبُّهُمْ بِإِيمَانِهِمْ ۖ تَجْرِي مِنْ تَحْتِهِمُ الْأَنْهَارُ فِي جَنَّاتِ النَّعِيمِ ﴿٩﴾ دَعْوَاهُمْ فِيهَا سُبْحَانَكَ اللَّهُمَّ وَتَحِيَّتُهُمْ فِيهَا سَلَامٌ ۚ وَآخِرُ دَعْوَاهُمْ أَنِ الْحَمْدُ لِلَّهِ رَبِّ الْعَالَمِينَ ﴿١٠﴾

سورة يونس الايتين [9-10]

List of contents

List of Tables

List of Figures

List of Symbols and Abbreviations

Symbol Physical	Meaning
Ct	Concentration after different time of irradiation
C.B	Conduction band
e/h+ pair	Electron-hole pair
eV	Electron Volt
XRD	X- ray diffraction
λ	Wavelength
V.B	Valence band
UV –Vis	Ultraviolet-visible
TEM	Transmission Electron Microscopes
hν	The photon energy
PDE	Photocatalytic Degradation Efficiency
NPs	Nanoparticles
nm	Nano meter
mW	Milli watt
C0	Initial Concentration
FE-SEM	Field emission scanning electron microscope
Eg	Energy gap
TGA	Thermal gravimetric analysis

C	Light speed
(λ max)	Maximum Wavelength
ZnO	Zinc oxide
CdS	Cadmium acetate
BG	Brilliant green dye

Abstract

In this study, ZnO-CdS nanoparticles were prepared using the Hydrothermal technique) at a temperature of 60 °C, and pH 6, the prepared samples were incinerated for one h at a temperature (500 °C). Also, (Pd doped ZnO-CdS) was prepared by photo deposition using an inert environment nitrogen gas .

The chemical and physical properties of the prepared nanocomposites were characterized using different techniques such as X-ray diffraction (XRD), transmission electron microscopy (TEM), Technique scanning electron microscope (FE-SEM), Thermal Gravimetric Analysis(TGA),and UV-visible. Results show doping Pd ions on the surface of ZnO-CdS, did not show any peaks for Pd in XRD characterization.

The UV-visible showed that the energy gap of ZnO-CdS was reduced from 3.42 eV to 2.98 eV after doping palladium nanoparticles. The photodegradation of brilliant green dye was studied using ultraviolet light under different conditions in the presence of Pd doped ZnO-CdS, studying the effect of factors such as the effect of dye concentration, The intensity of incident light,The mass of prepared nanocomposite and studying the , stability of ZnO-CdS/pd nanocomposites .It was observed that the photocatalytic degradation of BG dye were 86.6%- 95.8% for first, to four cycles. This indicates the good stability of ZnO-CdS/pd nanocomposites and could be potentially applied in practical batch degradation.

Removal of Pollutants (Dyes) by Using ZnO-CdS\Pd nanoparticles to treat water pollution through toxic textile dyes by taking a laboratory sample of a mixture with toxic textile dyes (100 ml) for a mixture of dye pollutants which gave a photocatalytic degradation 90% under optimum condition .

All experiment was performed at The utmost optimum condition BG dye concentration of 50 mg/L , light intensity (2.7 mW/cm2),and solution pH 6.8. The results showed that the efficiency of the Pd- doping ZnO-CdS surface increased by 86.6%. It also showed that the photocatalytic degradation rate increased with decreasing concentration of brilliant green dye, Increasing the intensity of the light led to an increase in the rate of photocatalytic degradation

1.0 Introduction

The industrial revolution changed the features of human life and brought about a qualitative shift in the economies of the countries of the world, which coincided with the call of Adam Smith - the most famous of the classical economists - in his book "The Wealth of Nations" to specialization and the division of labor, so the production process increased at unprecedented rates, but as everything has a cost, this came Economic progress and increased production at the expense of the environment have also increased pollution rates in an unprecedented way, and have reached the point of danger that they threaten the entire planet, especially with developing countries racing to move their production machinery to catch up with the major industrialized countries, in addition to that military machine and its harmful waste. Long lasting and difficult to process[1],[2]. What makes it difficult to reduce pollution or to find feasible ways and means to confront it is the conflict of international interests, in addition to the interdependence of environmental problems and their overlap with each other because of the inter linkages between pollution problems. This leads to an increase in pollution rates, and accordingly, people tend to devise effective solutions to preserve the environment, and here comes the role of nanotechnology and its applications as one of the innovative solutions that have shown remarkable effectiveness in treating some forms of pollution[3],[4]. For example: the issue of water purification comes on the list of human priorities due to its vital importance to human existence, as well as the scarcity of fresh water on the surface of this blue planet, and experiments have proven the effectiveness of some nanomaterials - especially granules of iron metal - in treating contaminated water and separating materials Toxic organic matter, when it is reduced to certain nanoscale dimensions[5], as well as groundwater treatment and sea and ocean water desalination, especially in countries that fall within the water poverty belt,

and nanomaterials - especially titanium dioxide powders - may be used to purify the air and manufacture more resistant materials. For bacteria, dirt, mildew and many other organic matter[6].

1.1 Nanotechnology

Nanotechnology is a multidisciplinary field originating from the interaction of several different disciplines, such as engineering, physics, biology and chemistry. New materials and devices effectively interact with the body at the molecular level, yielding a brand new range of highly selective and targeted applications designed to maximize therapeutic efficiency while reducing the side effects. Liposomes, quantum dots, carbon nanotubes and super paramagnetic nanoparticles are among the most assessed nanotechnologies. Meanwhile, other futuristic platforms are paving the way toward a new sc ientific paradigm, able to deeply change the research path in medical science. The growth of nanotechnology, driven by the dramatic advances in science and technology, clearly creates new opportunities for the development of the medical science and disease treatment in human health care. Despite the concerns and the on-going studies about their safety, nanotechnology clearly emerges as holding the promise of delivering one of the greatest breakthroughs in the history of medical science[7]

Nanotechnology refers to the branch of science and engineering devoted to designing, producing, and using structures, devices, and systems by manipulating atoms and molecules at nanoscale, i.e. having one or more dimensions of the order of 100 nanometers' (100 millionth of a milli metre) or less.In the natural world, there are many examples of structures with one or more nanometer dimensions, and many technologies have incidentally involved such nanostructures for many years, but only recently has it been possible to do it intentionally. Many of the applications of

nanotechnology involve new materials that have very different properties and new effects compared to the same materials made at larger sizes. This is due to the very high surface to volume ratio of nanoparticles compared to larger particles, and to effects that appear at that small scale but are not observed at larger scales[8-11].

1.2 Nanocomposite

A nanocomposite combines two or more materials – of which at least one is a nanomaterial – with different physical and chemical properties. Nanocomposite materials are designed to exhibit properties that exceed, sometimes drastically, the capabilities of the sum of their constituent parts. Nanocomposites are those composites in which one phase has nanoscale morphology like nanoparticles, nanotubes, or lamellar nanostructure. They have multiphases so are multiphasic materials, at least of the phases should have dimensions in the range of 10–100 nm. To overcome the limitation of different engineering materials now a days, nanocomposites are emerged to provide beneficial alternatives. Nanocomposites can be classified on the basis of their dispersed matrix and dispersed phase materials . With the help of this rapidly expanding field .Hence, the idea behind nanocomposite is to use building blocks with dimensions in the nanometer range to design and create new materials with unprecedented flexibility and improvement in their physical[12-14].

1.2.1 Types of Nanocomposites

Nanocomposite materials can be classified in the following way based on the presence or absence of polymeric material in the composite :

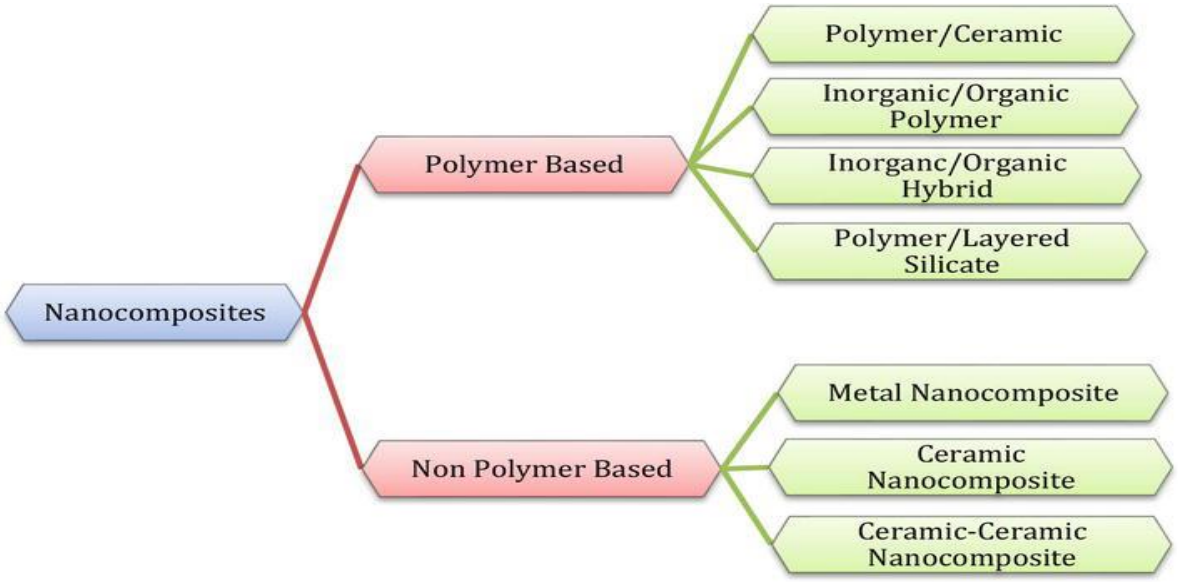

Fig 1.1: classification of nanocomposites[15]

1.3 Synthesis of nanoparticle(NP)

In nanoparticles synthesis, there are two primary approaches known as top-down and bottom-up. Top-down approach describes that NPs synthesis from bulk materials into smaller ones. Top-down strategy mostly falls under the physical method of NPs synthesis as it acquires big tube furnace to smash bulk material into smaller parts While bottom-up strategy suggests that NPs are synthesized to the required material from smaller molecules [16].

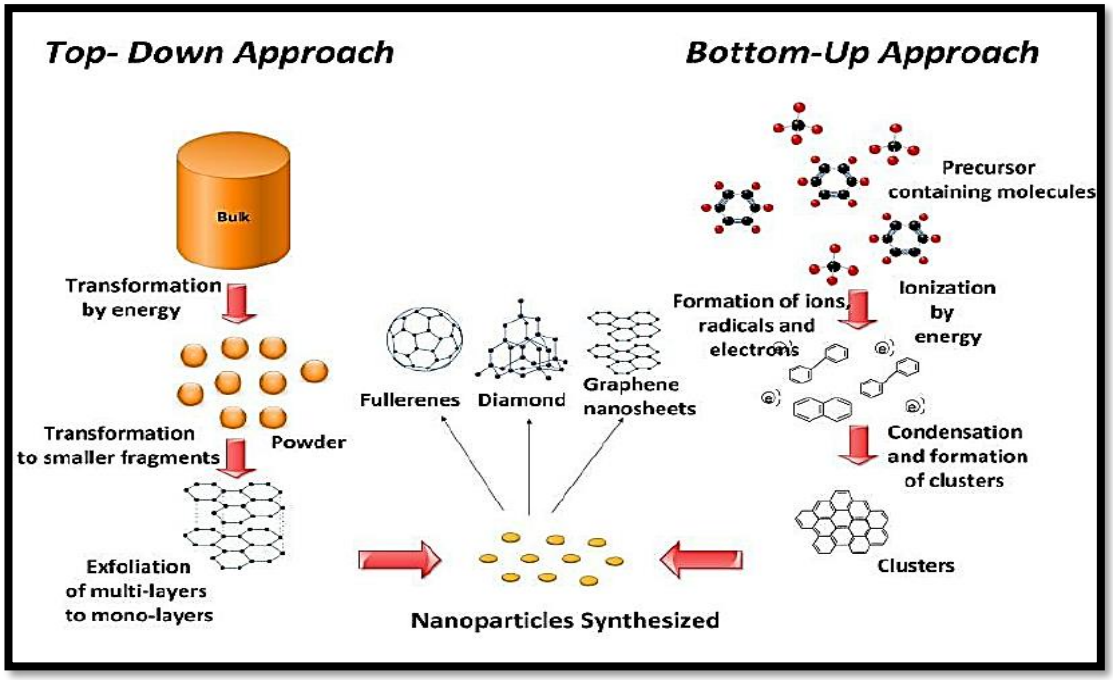

Fig1.2 :Schematic illustration of top-down and bottom-up approach in nanoparticle synthesis[17].

1.4 Applications of nanoparticles (NPs)

Regarding to the exceptional properties, NPs can be used in variety of applications of which:

1.4.1Applications in genetics and gene

Therapy magneto fiction is one of the applications of nanotechnology in which gene vectors, is combined with NPs (MNPs) to enhance gene transfer in the presence of a magnetic field . As an alternative to viral vectors, various NPs including natural polymers, natural inorganic particles, cationic lipids, dendrimers, polyethyleneimine derivatives, and carbon-based nanoparticles have been investigated for genetic material transfer to the central nervous system (CNS) in order to decrease toxicity and improve the efficiency of transfection through the enhancement of blood-brain barrier crossing which represent the main obstacle .Gold and silver hybrid nanoparticles (Ag/Au NPs) have also been used in tissue engineering, protein detection, cancer therapy, multicolor optical coding for biological assay at genome level . The use of

RNA based, antigen-free, 20-40 nm particles holds promise for the long term recurring treatment of chronic diseases. Researches get attention of RNA NPs fabrication to improve pathogen detection, drug/gene delivery, and therapeutic application [17-19].

1.4.2 Applications in drugs and medications.

Inorganic nanoparticles of either complex or simple nature, exhibit distinctive, physical and chemical characteristics and represent an progressively important material in the evolution of novel nanoscale devices which can be used tremendously in biological, biomedical, pharmaceutical and physical applications [20]. Nanoparticles (NPs) have drawn the attention by every branch of medicine for their ability to optimize drug delivery resulting in enhanced therapeutic efficiency of the drugs, weakened adverse effects and improved patient obedience. To overcome the microbial species selectively; These NPs functionalized with various groups. BiVO4, TiO2, Cu, ZnO, and Ni-based NPs have been employed for this purpose as a result of their suitable antibacterial efficacies[21] .

1.4.3 Applications in water treatment

Nanotechnology is now playing an important role in water treatment procedures. Nanotechnology is the manipulation of atoms on a nanoscale. Nanomembranes are used in nanotechnology to soften water and remove impurities such as physical, biological, and chemical contamination. There are several nanotechnology techniques that use nanoparticles to provide safe drinking water with a high level of efficacy. Some techniques have found commercialization. Nanotechnology is chosen for improved water purification or treatment methods[22]. In water treatment operations, many different types of nanomaterials or nanoparticles are used. Remediation, desalination, filtration, purification, and water treatment all

benefit from nanotechnology[23].The primary characteristics that make nanoparticles efficient for water treatment are as follows[24]:

- more surface area
- Small size, The greater the surface.

1.5 Zinc oxide

Zinc oxide (ZnO) is a wide band gap (Eg = 3.37 eV at room temperature, near-UV spectral region) semiconductor with high exciton binding energy (60 meV) enabling persistence of excitonic emission processes at or above room temperature . It has great potential for various applications, such as UV light emitters, photocatalysts, surface acoustic wave devices, piezoelectric transducers, optical waveguides[25] .Among metal oxides, ZnO is a prototypical n-type material with numerous applications, including catalysts, gas sensors, varistors, transparent electrodes, etc. Renewed interest has recently emerged for its ultraviolet light emission capabilities [26] . Progress towards ZnO-based optoelectronic devices and applications, however, has been impeded largely by unintentional and seemingly unavoidable n-type conductivity of ZnO materials that makes stable p-type doping extremely daunting. In order to solve this most puzzling problem for ZnO, it is highly desirable to understand the origin of the unintentional n-type conductivity[27]. ZnO has a good optical-transmission at both nearinfrared and visible-light areas because of its broad energy bandgap and the transmission percentage of the ZnO surface depends on their microstructure and roughness. The energy bandgap of ZnO can be shifting through extrinsic or intrinsic dopants. This shifting named the Burstein Moss effect [28]. When the charge carriers concentration increases the Fermi energy-level moves above CB edge, then the full occupation of states at the bottom of CB. Accordingly optically transitions (stimulated) from the VB to these states cannot occur, and the increases of

ZnO energy bandgap were investing. To increase "electricalconductivity" within ZnO the mobility and charge carrier concentration must be simultaneous[29]. These increases in the concentration of charge carriers can be done by applying two approaches (i) insert the intrinsic dopants (i.e. Ag, Fe2O3) in matrix or lattice of ZnO; also employed oxygen vacancies as defects in the structure (ii) introduction of "zinc lattice" sites atoms at "oxygen lattice" sites[30].

Table(1.1): Basic Properties of Zinc Oxid[31]

Parameter	**Value**
Band gap	3.37 eV (direct band gap)
Density	5.606 g. cm–3
Crystal structure	Wurtzite, rock salt and zinc blende
Stable phase at 300 K	Wurtzite
Appearance Amorphous	Amorphous white or yellowish white powder
Melting point	1975ºC
Nature of oxide	Amphoteric oxide
Exciton binding energy	60 meV
Ionicity	62%
Refractive index	2.0041
Solubility in water	0.16 mg 100 ml^{-2}

Relative dielectric Constant	8.66
Lattice constants at 300	a : 0.32495 nmc : 0.52069 n

1.5.1 Crystal structure of zinc oxide:

ZnO crystallizes in three forms :

1-Hexagonal Wurtzite

2-cubic zinc blende

3- cubic rock salt

Most of the group II–VI binary compound semiconductors crystallize in either cubic zinc blende or hexagonal wurtzite (Wz) structure where each anion is surrounded by four cations at the corners of a tetrahedron, and vice versa. This tetrahedral coordination is typical of sp3 covalent bonding nature, but these materials also have a substantial ionic character that tends to increase the bandgap beyond the one expected from the covalent bonding. ZnO is a II–VI compound semiconductor whose ionicity resides at the borderline between the covalent and ionic semiconductors [32].

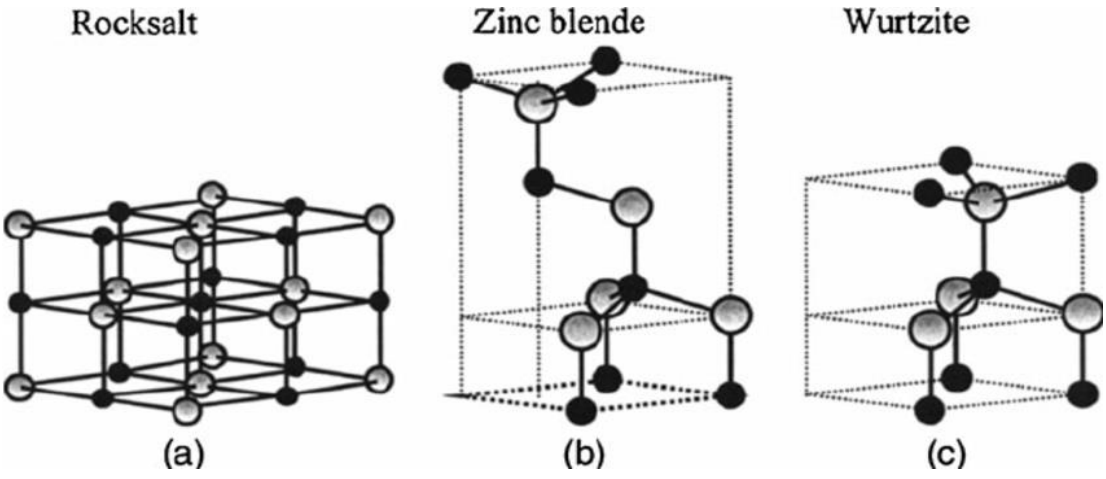

Fig1.3 :Stick-and-ball representation of ZnO crystal structures: (a) cubic rocksalt , (b) cubic zinc blende , and (c) hexagonal wurtzite . Shaded gray and black spheres denote Zn and O atoms, respectively[33].

1.5.2 Application of ZnO :

There are different application of Zno in different fielids of life as in below[34] :

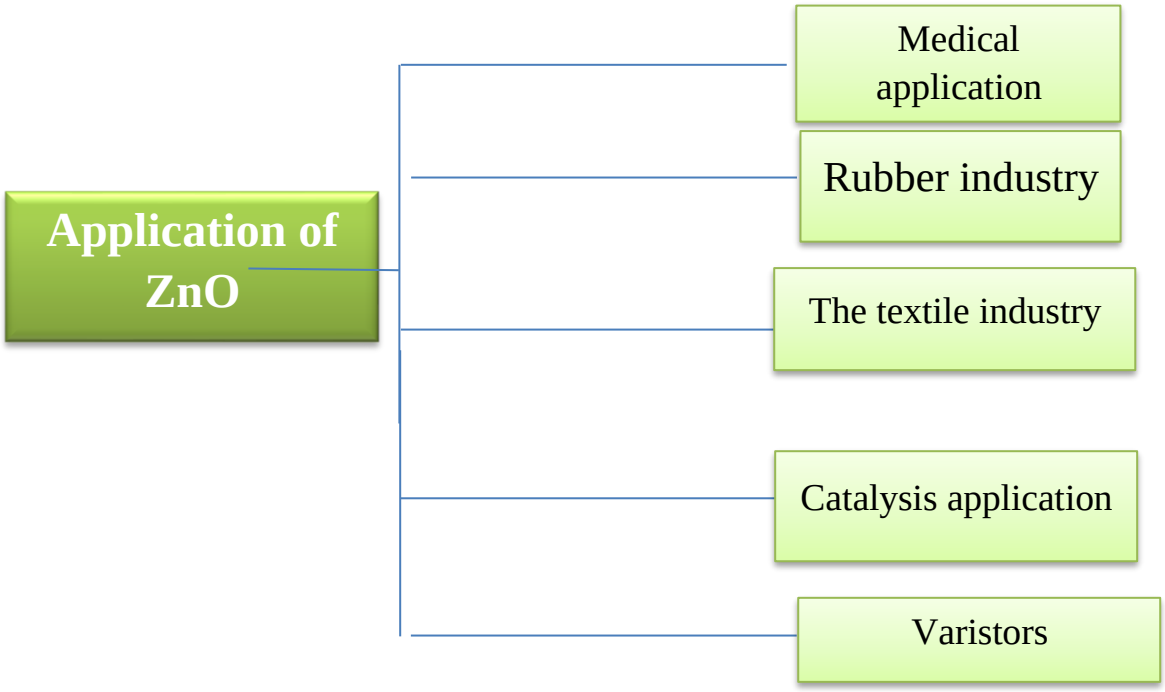

Fig 1.4 :Industiral Application of ZnO[35]

1.5.3 Synthetic Methods for ZnO Nanostructure

The zinc Oxide is synthesized by adopting different strategies, Such as solution-based synthesis and vapor-phase-based methods. It is worth noting here that synthesis methods can have a significant impact various parameters, such as particle size and crystallization. The solution-based synthesis methods are preferred for controlling the morphology and size of nanostructures by changing the solvent, precursor and reaction conditions, such as temperature, heating time, etc . The following are the main methods of synthesis of zinc oxide **.** Different synthesis methods have been devised their basic methods are shown in fig(1.5) .

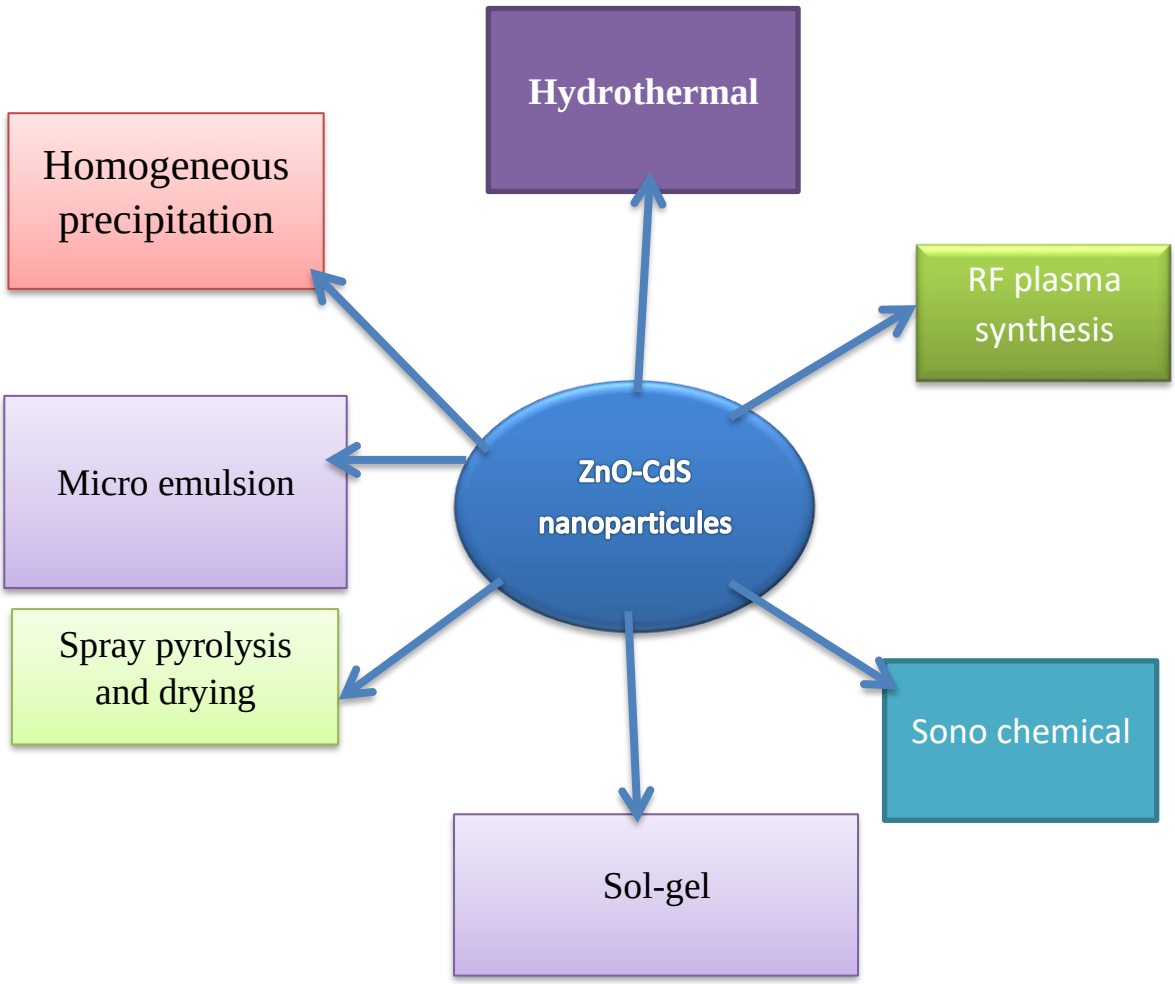

Fig.1.5: Flowchart main methods for preparation of ZnO nanoparticles[36]

1.6 Cadmium Sulfide

Cadmium Sulfide CdS is a semiconductor with a band gap of 2.42 eV and a maximum absorption peak of 514 nm wavelength which shows CdS can absorb visible light and UV light within a wavelength of ≤ 514 nm. This makes CdS an efficient photocatalyst. In addition, the bandgap position of CdS semiconductors is well suited for many photocatalytic reactions, such as water decomposition and CO2 reduction. The CdS has extensively been investigated as a photocatalyst. Of note, the position of the CdS conduction band edge is lower than the position of other common semiconductors such as TiO2, ZnO, and SrTiO3; this means in the photocatalytic reaction, the photoelectrons of CdS have a strong reducing power. However, the CdS

material is prone to corrosion by light. This causes limitations on the number of recoverable CdS photocatalyst. To solve this fundamental problem, researchers have proposed measures to improve the CdS photocatalyst is to use its ratio. The most commonly used method is to prepare CdS composite material is by using different materials or ion doping methods[12] ,[37] ,[38].

Table (1.2) Properties of Cadmium Sulfide[39]

Property	**Value**
Physical state and appearance	Solid. (Solid powder.)
Molecular Weight	144.46 g/mole
Color	Yellow or brown
Melting Point	Sublimes. (980°C or 1796°F)
Specific Gravity	4.82 g/cm^3
Solubility	Insoluble in hot and cold water

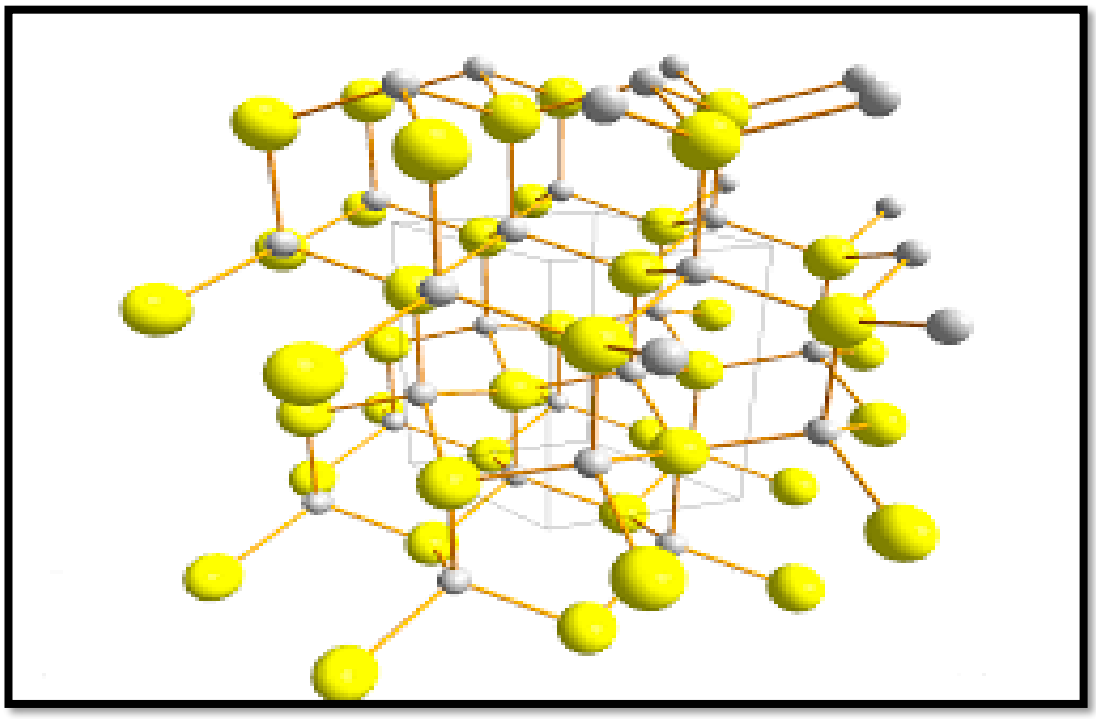

Fig 1.6: The crystalline structure cadmium sulfide[40].

1.7 Synthesis of ZnO-CdS Nanocomposite:

1.7.1 Hydrothermal synthesis

Hydrothermal synthesis is one of the most commonly used methods for the preparation of nanomaterials. It is basically a solution reaction-based approach. In hydrothermal synthesis, the formation of nanomaterials can happen in a wide temperature range from room temperature to very high temperatures. To control the morphology of the materials to be prepared, either low-pressure or high-pressure conditions can be used depending on the vapor pressure of the main composition in the reaction. Many types of nanomaterials have been successfully synthesized by the use of this approach. There are significant advantages of hydrothermal synthesis method over other[41]. Hydrothermal synthesis can generate nanomaterials which are not stable at elevated temperatures. Nanomaterials with high vapor pressures can be produced by the hydrothermal method with minimum loss of materials. The compositions of nanomaterials to be synthesized can be well controlled in hydrothermal synthesis through liquid phase or multiphase chemical reactions[42]. This special issue serves as a forum presenting the recent research results of hydrothermal synthesis of nanomaterials. Several papers on hydrothermal synthesis of nanoparticles, nanorods, nanotubes, hollow nanospheres, and graphene nanosheets have been published in this special issue. New synthesis methods, for example, microwave-assisted hydrothermal synthesis and template-free self-assembling catalytic synthesis, are reported in this special issue[43].

1 .7.2 Solvothermal Method

Solvothermal synthesis is similar to hydrothermal synthesis in that organic solvents are used instead of water. Solvothermal synthesis offers various advantages over other approaches. Solvothermal conditions allow for fast convection in solution[44] . The relatively mild environment provides conditions for the formation

of crystals with few lattice defects, as well as fine control over the size, shape distribution, and crystallinity of nanoparticles. The low boiling point of the organic solvent involved can give a larger reaction pressure when the technique of crystallization is carried out at high temperatures. Because of the mild temperature, specific structural properties of precursors can be transferred to products, allowing for control of product morphology. Solvents can also provide functional groups, which can be used in other ways[45]. solvothermal synthesis can reduce the releasing of harmful vapour during the reaction. The sealed system not only contributes to carry out green chemistry, but also efficiently reduces the possibility of oxidation and contamination from atmosphere or oxygen, an important point for high purity products. Finally, in order to control the size as well as the shape of nanoparticles synthesized[46].

1.7.3 Method of Precipitation

The precipitation method is defined as a chemical reaction that occurs in an aqueous solution and results in the creation of an insoluble salt. Precipitates are insoluble salts generated during precipitation reactions. Precipitation reactions are often double displacement events that result in the formation of a solid form residue known as the precipitate. When two or more solutions with different salts are mixed, these reactions occur, resulting in the creation of insoluble salts that precipitate out of the solution[47].

1.8 Advance Oxidation Process (AOPs)

The term "advanced oxidation processes" (AOP) describes a group of chemical treatment techniques used to oxidize organic (and occasionally inorganic) compounds in water and wastewater. These reactions take place in the presence of hydroxyl radicals. These oxidation techniques may effectively eliminate all

contaminants, even those with minimal reactivity, and mineralize them thoroughly[48].AOPs, which include wastewater treatment methods including Fenton, ozonation, Sono lysis, photocatalysis, UV photocatalysis, and wet air oxidation, constitute the foundation of environmental remediation science today. Complete degradation of many kinds of pollutants is provided by these AOPs. AOPs are a group of chemical treatment methods used in environmental engineering that are intended to oxidize organic and occasionally inorganic contaminants from water and wastewater through interactions with hydroxyl radicals (OH). This term typically refers to a subset of chemical species that use UV, hydrogen peroxide, and ozone in the wastewater treatment field[49], [50].

Advanced oxidation processes have become a crucial part of the wast water treatment process. The majority of wastewater treatment methods are physicochemical in nature, using either physical or chemical processes or a combination of the two. AOPs, one of the most sophisticated techniques, are founded on a fundamental idea that calls for the creation and application of a Strong oxidants like the hydroxyl free radical (HO*) can be used to break down substances that can't be broken down by other types of oxidants. Due to its exceptional effectiveness, AOPs have demonstrated premises in different water treatment industries[51].

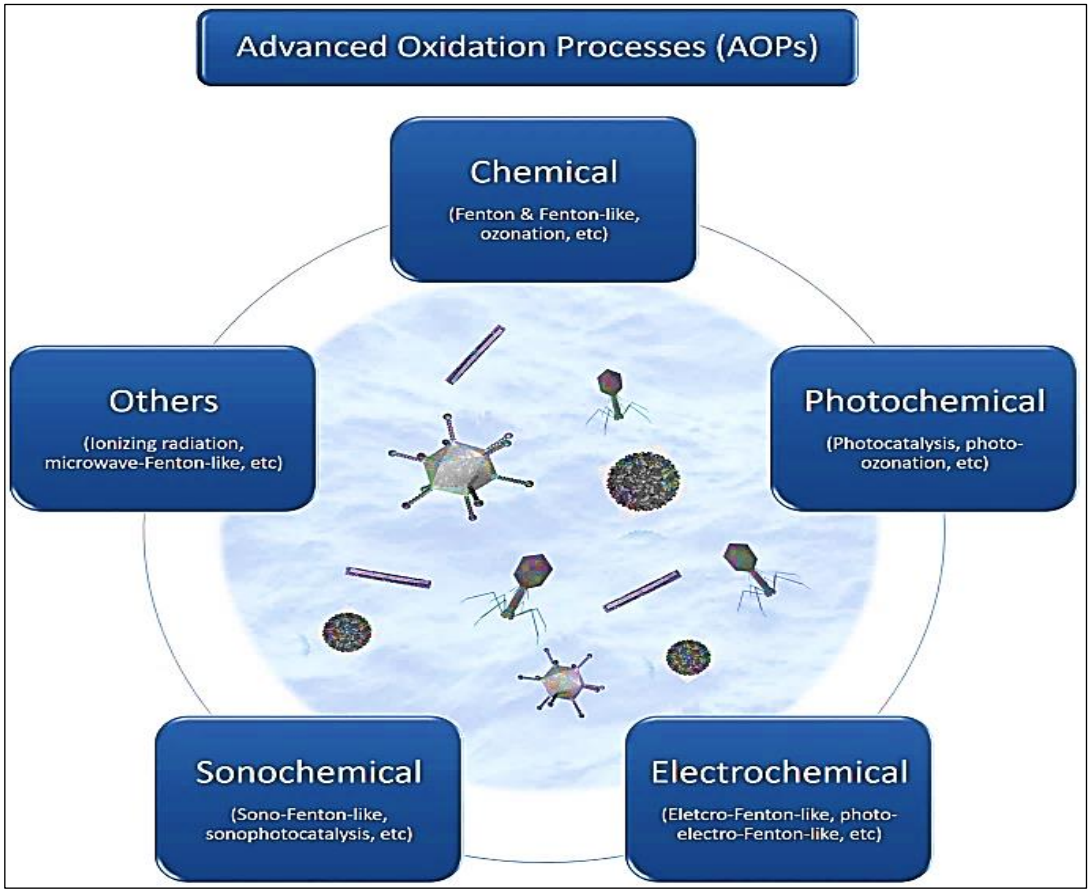

Fig .1.7 Classification "advanced oxidation processes" (AOP)[53].

1.9 Photocatalytic degradation

Photocatalysis is a reaction in which near ultraviolet light (380 nm) is used to excite a semiconductor photo catalyst in the presence of oxygen, and the photo catalyst alters the reaction without being consumed as a reactor. The kind and size of photocatalyst have a significant impact on photocatalysis[52]. The band gap energy required to activate the catalyst should be proportional to the wavelength of the light source. The specific surface area of photo catalyst lighted and photo catalyst contact area decrease as size decreases reaction medium increases.Under UV light, Muller discovered that ZnO could degrade isopropanol. This finding proved photocatalysts' ability to destroy organic compounds in water. Since then, countless scientists have dedicated their time and effort to photocatalytic research, boosting photocatalytic

efficiency and broadening the variety of photocatalytic devices and applications [53]. Semiconductors are the most essential photocatalyst materials because they have a valence band (full electron) and a conduction band (higher energy and no electron) with a clear band gap. The basic principle of the photocatalytic process is that when photons from a light source with energy (h) larger than or equal to the band gap energy (Eg) of ZnO catalyst shine on it, electrons from the valence shell are activated from the valence band (VB) to the conduction band (CB) region, leaving holes in the VB. This creates electron hole ($e^-/h+$) pairs.as shown in Fig(1.4).

$$ZnO + h\nu \rightarrow ZnO\ (e^-/h+) \quad (1\text{-}1)$$

Dye molecules absorb photons and get energetically excited from their highest occupied molecular orbital (HOMO) to lowest unoccupied molecular orbital (LUMO)

$$Dye + h\nu \rightarrow Dye^* \quad (1\text{-}2)$$

Then, the photo excited electrons diffuse on to the surface of the catalyst and react with adsorbed oxygen, reducing it to superoxide radical ion ($O2^-$).

$$e^- + O2 \rightarrow O2 \quad (1\text{-}3)$$

The dye was then oxidized to cationic radicals.+ By introducing LUMO electrons to the CB of the semiconductor or to oxygen dissolved in solution .

$$O2 + Dye^* \rightarrow O2^- + Dye+ \quad (1\text{-}4)$$

while the holes move to the surface and react with neighboring adsorbed H2O or dye molecules, oxidizing them to hydroxyl radical ($OH^{\cdot}$) .

$$H2O + h+ \rightarrow OH^{\cdot} + H^+ \quad (1\text{-}5)$$

and oxidized dye radical cation (dye+).

$$Dye + h+ \rightarrow dye+ \quad (1\text{-}6)$$

It is mainly due to the formation of the reactive hydroxyl and superoxide radicals in the solution that set in a chain of catalytic reactions leading to the eventual degradation of the dye in to CO2, H2O, and few mineral acids .

$$\text{Dye} + OH^{\cdot} \text{ or } O2^{-} \rightarrow \text{Degraded products} \quad (1\text{-}7)$$

The (e/h +) pairs on the ZnO catalyst's surface undergo crucial redox events that contribute to their separation, speeding up the pace of degradation. Rapid recombination, on the other hand, slows down the creation of radicals and the pace of degradation. Coupled with surface flaws in ZnO catalysts that serve as trapping foci for holes and electrons, oxygen in the solution serves as a scavenger for excited VB electrons, which limits pair recombination and may increases degradation[54].

Used nano-semiconductors including TiO2, ZnO, SiO2, Fe2O3, CdS, ZnS, etc. increasingly to satisfy some environmental issues by several applications including solar cells, water splitting, sensors, and so on. Semiconductors must have the following properties: (i) photo responsiveness, (ii) chemical, biological, and light corrosion stability, (iii) high activity in the UV-vis region, (iv) low cost, and (v) no toxicity it in comparison to the other approaches[55-57].

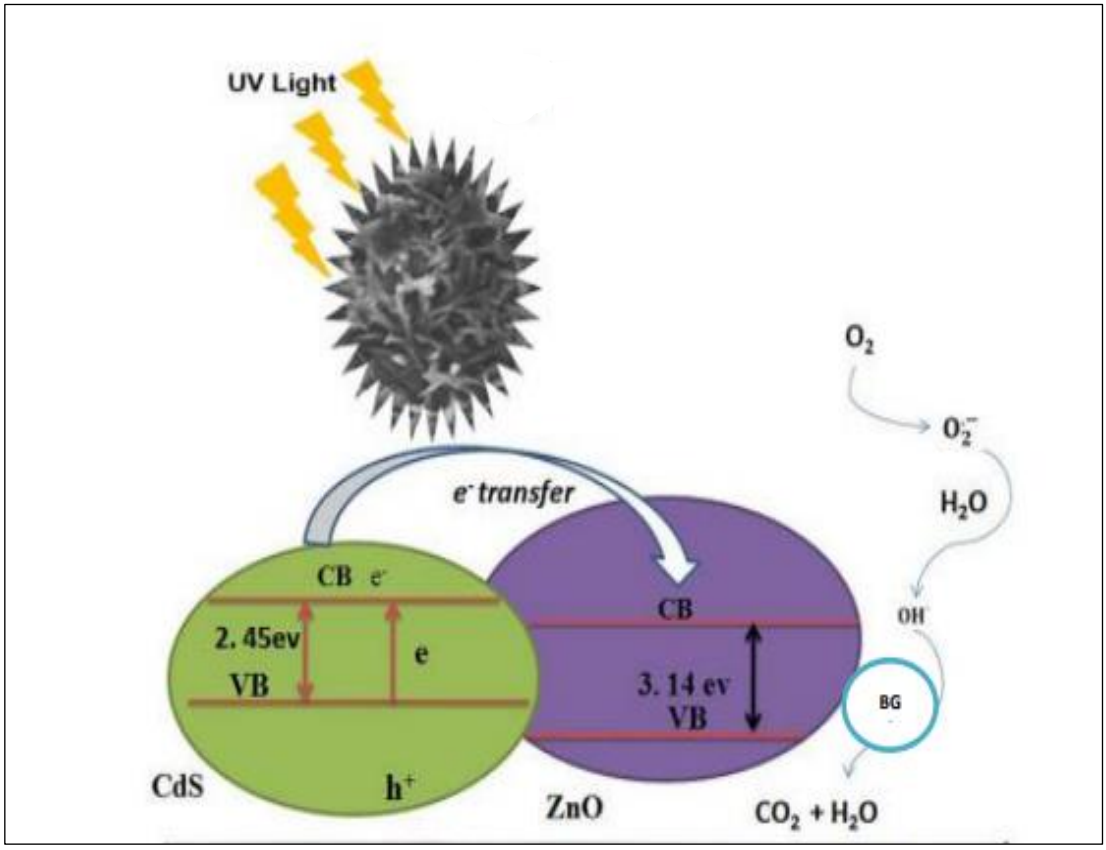

Fig.1.8 Mechanism for Photocatalytic Degradation of Dyes .

1.10 Literature Review

Yin, X., et al developed Ag-ZnO nanocrystals via an uncomplicated hydrolysis method of zinc acetate dihydrate with a modification of Ag+ (ions) in the "di ethylene glycol". To form an effective contact between ZnO and Ag the sodium hydroxide (NaOH) with various molarities was added in the above mixture. The influences of NaOH content on both morphological and structural characteristics were discussed. The photocatalytic activity outcomes showed good degradation to the methyl orange (MO) aqueous solution under ultraviolet irradiation because of morphology and composition of the resulting NPs, which were attributed to formed the "heterostructure" between ZnO and Ag[58].

Hydrothermal method is an effective route to synthesize CdS nanoparticles with good crystallinity and having average grain size of about 12 nm. The results show that samples sintered by small amount of CdS nanoparticles (≤ 0.3 wt%) exhibit the higher critical current densities and energy pinning in applied magnetic fields compared to free added sample. Consequently, the addition of CdS could introduce effective pinning centers which account for the improvement in superconducting properties in the Bi-2223 materials[59]

In this work, ultrathin agaric-like ZnO nano sheets were successfully fabricated by a simple one-step hydrotherm al method. Pd modified ultrathin agaric-like ZnO nanosheets were obtained successfully through calcination. Pd-ZnO-0.3 sensors exhibit sensing performance to aniline gas with high response, excellent selectivity and low detection limits. The surface morphology, crystal structure and chemical element properties of Pd-ZnO nanomaterials were characterized, and the sensing mechanism of Pd-ZnO nano materials for aniline was systematically validated by DFT study. In general, Pd-decorated ultrathin agaric-like ZnO nanosheets were successfully prepared by one-step hydrothermal method as a chemical sensor for the aniline detection. The Pd-ZnO-0.3 sensor exhibited excellent gas sensitivity and selectivity to aniline compared to the intrinsic ZnO sensor. In addition, the Pd-ZnO-0.3 aniline sensor has the advantages of low detection limit, excellent stability and short recovery response time[60]

Cadmium sulfide CdS nanoparticles were synthesized in aqueous medium at pH constant, the obtained nanoparticles has been characterized by x-ray diffraction (XRD) and transmission electron microscopy (TEM), It was found that CdS nanoparticles showed relatively higher antioxidant activities that this nanomaterial' scan reactat the interface with the life entities. CdS nanoparticles with average grain

size of about 12 nm were successfully synthesized by hydrothermal method. The results presented highlight the possible uses of CdS nanoparticles in different biological level of study. Our results aimed to show the antioxidant activity in vitro of new compound (Cd-S). Our data showed that compound complex has an antioxidant character; this is demonstrated by scavenging DPPH radicals, ABTS radicals, hydroxyl radical scavenging and reducing property to that of ascorbic acid [61]

The photocatalytic decolorizations of aqueous solutions of Reactive Red 2 dye in the presence of ZnO suspension has been investigated with the use of artificial UV-A light sources. The effects of various parameters, such as time of irradiation, photocatalyst amount, pH, addition of H2O2 and temperature on photocatalytic degradation were investigated. The decolorization is not feasible in the absence of catalyst, oxygen and/or irradiation. The decolorization process of the dye follows pseudo-first order kinetics.The photocatalytic decolorization of Reactive Red 2 dye proved that the reaction obeys the pseudo first order, and the optimum conditions such as ZnO concentration, pH, temperature and addition of H2O2 of photocatalytic decolorization of this dye were investigated. The best dosage of ZnO found at 2.5 g/L, because the active sites of ZnO surface is propionate to this reaction [62]

Hydrothermal method has been attracted many researchers because of its distinct advantages like simple equipment, low cost and mild preparation conditionsIn this work we mainly emphasize the effect of reaction parameters on structural and optical properties of nanoparticles. Here hydrothermal reaction time is varied from 1 h to 5 h and temperature from 100 °C to 150 °C. Ph of solution mixture is kept as 12 to understandits influence on nanomaterial growth Here nanoflowers and nanorods are showing excellent photoluminescence, UV absorption and suitable bandgap. Nanorods are thermally stable than nanoflowers. Optical properties and thermal

stability are the key factors for solar cell materials. Based on their optical properties and thermal stability we can propose these hydrothermally synthesised nanorods and nanoflowers for different layers of solar-cell[63]

Experiment performed under visible light source also showed that CuS could aid ZnO in the degradation of Congo red and Phenol. From the UV analysis it was found that CuS/ZnO nanocomposite exhibits better photochemical stability. All of these results suggested that prepared sample could be useful in practical applications. CuS/ZnO was successfully synthesized by grinding the ZnO and CuS, which were synthesised by using the precipitation method. CuS precisely existed in the nanocomposite particles, according to SEM images and XRD analysis. The nanocomposite's average size was around 35 nm. Cyclic voltammetry and electrochemical impedance spectra were used to evaluate the electrochemical study of CuS/ZnO. Under visible light irradiation, the CuS-modifying ZnO can function as an outstanding improved photocatalyst [64]

In the present work a cheap chemical bath deposition technique has been employed to prepare Ni-doped CdS (Ni: CdS) thin films and Ni: CdS/p-Si hetero junctions using different Ni concentrations varied from 0 to 7 wt %. The X-ray diffraction study confirms the cubic crystal structure for CdS and Ni: CdS thin films. The linear optical parameters of the CdS and Ni: CdS thin films were estimated via the transmission and reflection measurements at the wavelength range 400–2500 nm. The enhancement of the electrical performance of CdS is very important to point gaining importance in recent years to improve the efficiency of the solar cell and optoelectronic devices. This improvement occurred by making a doping process for the CdS thin film with a metal atom to produce low resistivity CdS thin films .High-quality CdS and Ni-doped CdS thin films were synthesized onto a pre-cleaned p-Si substrate and glass

substrate by a low-cost chemical bath technique. The XRD studies revealed that all the CdS and Ni-doped CdS thin films exhibit a cubic crystal structure. The optical analysis of the CdS and Ni-doped CdS thin films indicate that the refractive index of the investigated films gradually increases with the increase in the Ni content. The CdS and Ni-doped CdS thin films exhibit a direct energy [65]

ZnO NPs, CdS NPs, and ZnO–CdS NCs are prepared by a simple chemical precipitation route and examined by a series of characterization techniques. The structural analysis demonstrated that the ZnO–CdS NCs exhibited a mixed phase for both hexagonal ZnO NPs, and CdS NPs with average crystallite size of 27 nm. Furthermore, the morphological studies reveal that ZnO NPs exhibited irregular and spherical-like structures, whereas CdS NPs only exhibit spherical-like structures. Optical absorption spectra confirm that the bandgap energy of ZnO–CdS NCs is well tuned by the decoration of CdS NPs on ZnO NPs surface. The suppressed PL intensity of ZnO–CdS NCs indicating that the reduction in recombination rate of photoinduced e−/h+ pairs resulted in enhanced photocatalytic activity. Under solar light, the ZnO–CdS NCs displayed a photodegradation efficiency of 98.16% towards RhB dye, which is 5.09 and 3.25 times that of pure ZnO NPs and CdS NPs, respectively. After four trials, the structural stability of ZnO–CdS NCs was verified[66].

ZnO/CdS composite was prepared using a simple one-step hydrothermal method, and its photocatalytic performance was investigated under different conditions. The photocatalytic efficiency of ZnO/CdS was 6345.04($\mu mol \cdot g^{-1} \cdot h^{-1}$) in H2 production from water splitting using Na2S and Na2SO3 as sacrificial agents. The photocatalytic efficiency of eosin Y-sensitized ZnO/CdS was 6939.39 ($\mu mol \cdot g^{-1} \cdot h^{-1}$) when triethanolamine was used as a sacrificial agent. The photocatalytic activity of ZnO/CdS was better than those of pristine ZnO and CdS

during H2 evolution. The ZnO/CdS composite also exhibited superior photocatalytic activity compared to pristine ZnO and CdS in the degradation of a mixed dye pollutant. The degradation rates of methylene blue, rhodamine B, and orange G in the mixed dye after 120 min of irradiation were 99.41 %, 92.96 %, and 65.74 %, respectively. Possible mechanisms for photocatalytic H2 production and photocatalytic degradation of organic pollutants have been proposed [67].

Photocatalytic degradation of Congo red was investigated using ZnO–CdS core–shell nano-structure coated on glass by Doctor Blade method in aqueous solution under irradiation. Field-emission scanning electron microscopy (FESEM) and X-ray diffraction (XRD) techniques were used for the morphological and structural characterization of ZnO–CdS core–shell nanostructures. XRD results showed diffractions of wurtzite zinc oxide core and wurtzite cadmium sulfide shell. FESEM results showed that nanoparticles are nearly hexagonal with an average diameter of about 50 nm. The effect of catalyst loading, UV-light irradiation time and solution pH on photocatalytic degradation of Congo red was studied and optimized values were obtained. Results showed that the employment of efficient photocatalyst and selection of optimal operational parameters may lead to complete decolorization of dye solutions. It was found that ZnO–CdS core–shell nano-structure is more favorable for the degradation of Congo red compare to pure ZnO or pure CdS due to lower electron hole recombination. The results showed that the photocatalytic degradation rate of Congo red is enhanced with increasing the content of ZnO up to ZnO(0.2 M)/CdS(0.075 M) which is reached 88.0% within 100 min irradiation[68]

ZnO nanoplates were synthesized by microwave-hydrothermal methods. Pd doped ZnO photocatalysts were prepared by microwave irradiation, UV irradiation, and borohydride reduction methods. The Pd/ZnO photocatalysts were characterized

by field emission scanning electron microscopy (FESEM), X-ray diffraction (XRD), energy dispersive spectroscopy (EDS) and UV–vis spectrophotometry. The obtained FESEM results confirmed the dispersion of Pd nanoparticles on the surface of ZnO nanoplates. The optical band gap value was calculated as 3.25 eV from UV–Vis diffuse reflectance spectra of ZnO and different Pd/ZnO photocatalysts. Since the preparation method of the photocatalyst is of great importance for determining the photocatalysis, the effect of this on photocatalysis was investigated. The results of the photocatalytic degradation of congo red in aqueous solutions under the UV-light showed that Pd/ZnO prepared by borohydride reduction method exhibited higher photocatalytic activity than the other ones. A plausible mechanism for the enhanced photocatalytic activity by Pd doped ZnO was proposed. The kinetics of photodecomposition of congo red, and the identification of photoproducts were investigated by using liquid chromatography–mass spectrometry (LC–MS). The possible photodegradation pathway of Congo red was also proposed according to the structures of the photoproducts obtained from LC–MS data [69]

1.11 The aim of the Study

In order to investigate the reaction behavior of the synthesis of the ZnO-CdS nanoparticles as optical and photocatalytic, this study has been set to achieve the following:

1. Preparation of pure ZnO-CdS nanoparticles by the Hydrothermal method.
2. Preparation of ZnO-CdS\Pd nanoparticles by photodeposition.
3. Investigation of the characterization of nanocomposite using different instrument such as XRD.
4. Using FE-SEM and TEM techniques to investigate of structural, surface , morphology and optical properties .
5. Studying photocatalytic activity under different conditions such as the concentration of the Nano-compound, catalyst concentration of pollutants and light intensity.
6. Role of doping Pd on the surface of ZnO-CdS to enhance the activities of Binary nanocomposites in the photocatalytic degradation of brilliant green dye
7. Reusability and stability of the Pd -doped ZnO-CdS nanocomposites

2.0 Materials and Methods

This chapter focuses on the description of the preparation of ZnO nanoparticles by hydrothermal technique , preparation of ZnO-CdS nanoparticles by hydrothermal technique and dopant metal (Pd) on ZnO-CdS nanoparticles by photochemical deposition, thechemicals used in this work, theapparatus and then discusses what diagnostic tools to use to examine these parameters.

2.1 Chemicals

The chemicals used in this work are listed in Table 2.1 All chemicals were used without further purification.

Table 2.1: Chemicals for all component

N0	Chemicals	Chemical formula	Supplier
1	Zinc acetate	$Zn(CH_3COO)_2$ .2H2O	alpha-chemika
2	Oxalic acid	$H_2C_2O_4$	alpha- chemika
3	Methanol	CH_3OH	alpha- chemika
4	cadmium acetate	Cd(CH3COO)2·2H2O	Qualikems
5	Silver nitrate	$AgNO_3$	Sigma-
6	Sodium sulfide	Na_2S	India
7	Pd chloride	Pd Cl_2	Sigma- Aldrich
8	Hydrogen Peroxide	H_2O_2	India

2.2 Instruments and Equipment

The instruments used in this study with their company are listed in table (2.2).

Table 2.2: The list of Instruments was used in this project.

No.	Instrument	Company supplied	Location of current measurement
1	UV-Visible spectrophotometer, Single beam	Shimadzu, Japan	University of Babylon / College of science for women
2	UV-Visible spectrophotometer, Double beam	Shimadzu, Japan	University of Babylon / College of science for women
3	Band gap energy measurement	UV/ Visible Shimadzue 2700	University of Babylon / College of science for women
4	LED/ UVA specific wavelength 365 nm	USA/ Thorlab company	University of Babylon / College of science for women
5	Field-Emission Scanning electron microscope (FE-SEM)	TESCAN ,Czechia Republic	University of Tehran
6	Transmission electron microscope (TEM)	Leo, Germany	University of Tehran
7	X-Ray diffraction (XRD)	Japan	The Ministry of Science and Technology , University of Tehran
8	Fourier – Transform (FTIR)	Shimadzu, Japan	Al-Muthanna University\ College of science
9	Thermal gravimetric analysis(TGA)	Japan	University of Babylon /College of science for women
10	Hydrothermal System	Germany	University of Babylon /College of science for women

11	Centrifuge	JANETZI - T5, Belgium	University of Babylon / College of science for women
12	Ultrasonic cleaner (power sonic 420)	Hwashin, Korea	University of Babylon / College of science for women
13	Oven	Labtech, Korea	University of Babylon / College of science for women
14	Sensitive balance	Denver instrument , Germany	University of Babylon / College of science for women

2.3 Preparation of Nanomaterials

2.3.1 Preparation of Zinc Oxide Nanoparticles

The Hydrothermal method was used to prepare ZnO nanoparticles . Firstly, in a beaker dissolve 4 gm of zinc acetate in 75 ml of distilled water, and in another beaker dissolve 5 gm of Oxalic acid in 75 ml of distilled water. Then mix the two chemical compounds above with the series of chemical reactions that takes place. The complete hydrolysis of zinc acetate with the Oxalic acid $H_2C_2O_4$ in water should result in the formation of a ZnO colloid. The resulting solution was transferred into the the Teflon cup was sealed stainless steel (the autoclave). After that ,the autoclave was placed inside the oven and the temperature of oven was set to 150c for 24 h .

2.3.2 Preparation of ZnO-CdS nanocomposite

The hydrothermal system used for preparing the nanocomposite (ZnO-CdS) appears in Figure 1. Oxalic acid (8 g), zinc acetate (5 g), cadmium acetate (2 g), and sodium sulfide (1 g) are mixed for 30 minutes before being introduced to a hydrothermal system and heated to 160 °C for 24 hours in an autoclave. To create the powder (ZnO/CdS) nanocomposite, the yellow powder precipitate was filtered,

washed with DW several times, and dried for 24 hours at 60 °C. a previously known method that was used to make ZnO-CdSNCs. The reaction process for the creation of ZnO-CdS NCs is as follows.

$$ZnO + (CH_3COOH)_2 + H2O \rightarrow Zn(CH_3COO)_2.2H2O + NaOH$$

$$Cd(CH_3COO)_2.4H2O + Na_2S + ZnO + H2O \rightarrow ZnO\text{-}CdS\ (CH_3COOH)_2 + 2H_2O + NaOH$$

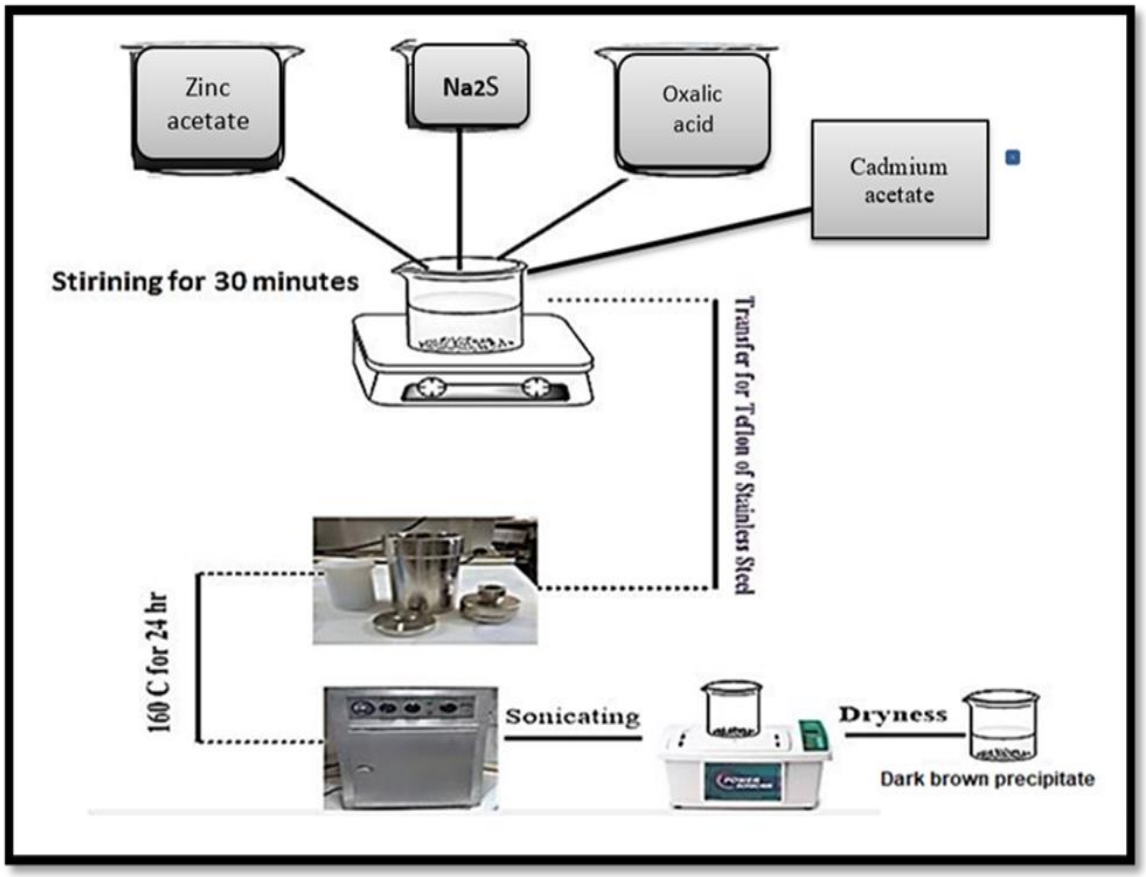

Scheme 2.1: Preparation of ZnO-CdS nanocomposite

Note:- The composite ZnO-CdS were prepared with different weights of cadmium acetate, while keeping the weights of the materials used in the preparation itself, and after conducting several tests to find out the efficiency of the surface on the dye BG, and the results were reached that the weight of a 2gm of cadmium acetate is the most efficient for the prepared surface . The weights were used in the following order:

1. 4.5 of cadmium acetate ZnO-CdS NPs1,
2. 2gm of cadmium acetate ZnO-CdS NPs 2,
3. 1gm of cadmium acetate ZnO-CdS NPs

2.3.3 Preparation of ZnO –CdS/ pd nanocomposite

To deposite of pd onto ZnO –CdS nanocomposite pick 0.5 g of Yellow nano-powder ZnO –CdS and (pdCl2) 0.05 % place them in a cell quartz (v/v 1% methanol/ deionized water) with 100 ml of with stirring, followed by exposing the surface of the mixture to nitrogen gas for 10 minutes under continuous magnetic stirring, ultra-sound moving the solution for a while then irradiated it for 10-12h under ultraviolet light (major wavelength 365 nm, L.I. 23 mW/cm) with uninterrupted stirring The powder was washed different times with DW by ultra-sound dried and dry at 65^{o}C for 24hr to obtain nanocomposite as show in Fig 2.2.

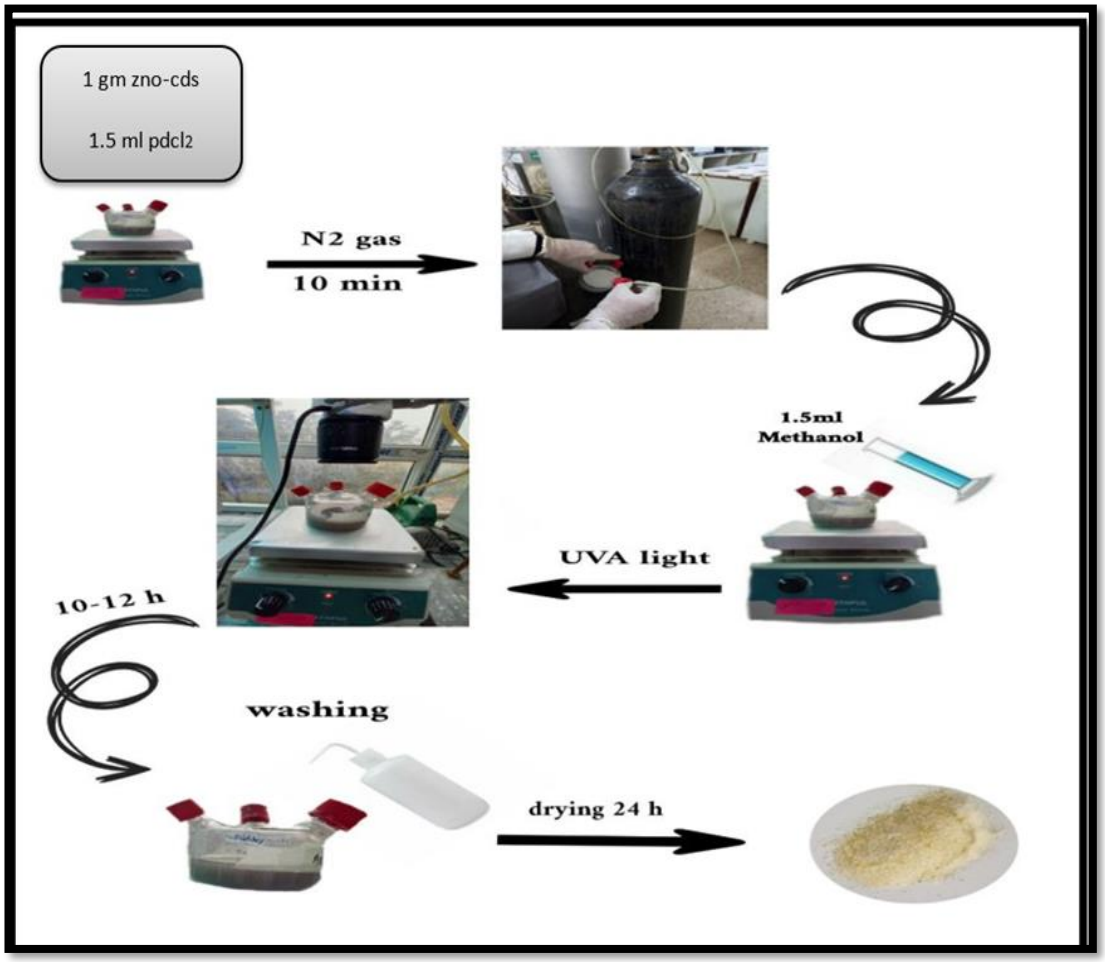

Fig 2.2 :Preparation of Pd\ZnO-CdS Nanocomposites

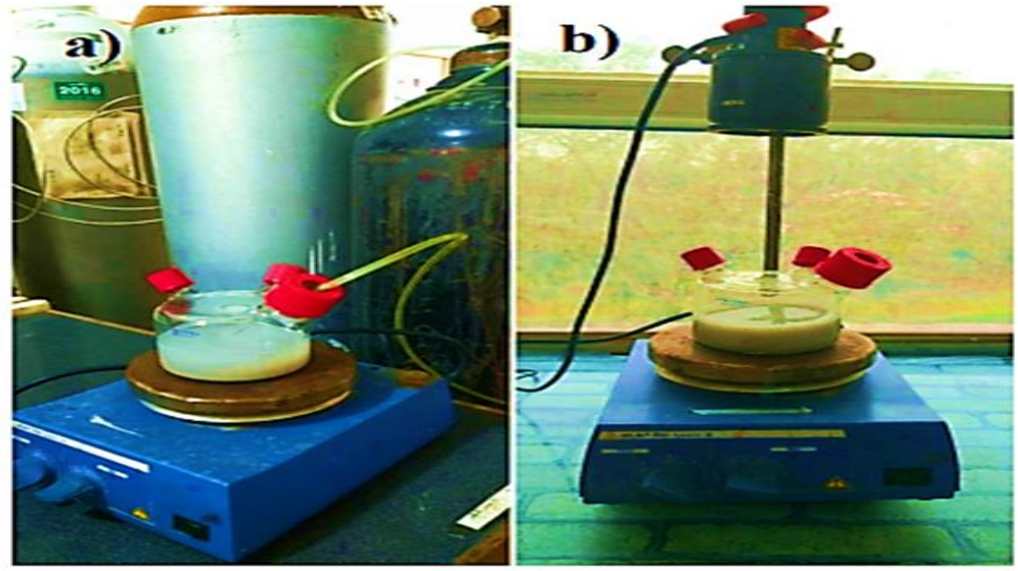

Fig 2.3: Real image for the photodeposition of pd doped ZnO-CdS (a) pugulate the mixed surface to nitrogen gas (b) Irradiate the mixture with a lamp LED

2.4 Characterization Techniques

"The majority of the analyses (FE-SEM,TEM, and XRD) took place at the University of Tehran, Iran. The rest of the analyses (UV-vis and TGA) were carried out in a college of science, at the University of Babylon, Iraq"

2.4.1 X-Ray Diffraction (XRD

A effective nondestructive technique for characterizing crystalline materials is X-ray diffraction. Utilizing a single wavelength of light (1.5104 nm) from a CuK source and nickel as a filter, the crystalline characteristics of materials created via an X-ray deflection approach were examined. Where the measurement's range (10–80 degrees) is derived from deviation angles [70]. It is importance to remember that the Scherer equation is only applicable to average diameters up to approximately 100 nm. Because the diffraction peak amplitude decreases with crystal size, it also depends on the instrument and the interaction between the signal and the sample with background noise. It can be quite challenging to separate and distinguish between crystal size-

related growth and expansion caused by other causes and components. Errors exist in all calculations, and successful calculation techniques are those that can minimize errors as effectively as possible to produce more accurate data[71-73]. .

2.4.2 UV-Visible Spectroscopy

The ultraviolet-visible (UV-Vis) spectrophotometer is an instrument commonly used in the laboratory that analyzes compounds in the ultraviolet (UV) and visible (Vis) regions of the electromagnetic spectrum. Unlike infrared spectroscopy (which looks at vibrational motions), ultraviolet-visible spectroscopy looks at electronic transitions. It allows one to determine the wavelength and maximum absorbance of compounds. From the absorbance information and using a relationship known as Beer's Law ($A = \varepsilon bc$, where A = absorbance, ε = molar extinction coefficient, b = path length, and c = concentration), one is able to determine either the concentration of a sample if the molar extinction coefficient is known, or the molar absorptivity, if the concentration is known (Wade 676-681). Molar extinction coefficients are specific to particular compounds, therefore UV-Vis spectroscopy can aid one in determining an unknown compound's identity. Furthermore, the energy of a compound can be ascertained from this technology by using the equation

$$E = hc/\lambda$$

(where E = energy, h = Planck's constant, c = speed of light, and λ = wavelength). Since photons travel at the speed of light, and h and c are constants, one can find the energy (Wade 501)[74],[75] .

Fig .2.7 A photo of ultraviolet-visible spectroscopy

2.4.3 Field Emission Scanning Electron Microscopy Analyzes (FE-SEM)

The field emission scanning electron microscope (FE-SEM) is a powerful tool for assessing sample morphology such as grain size, particle size, particle distribution, crystal defects, and surface structure. The FE-SEM has various advantages, including a large depth of field, higher resolution, and greater control over the degree of amplification. A 50L sample suspension in water or ethanol was deposited on a clean silicon wafer surface. The solvent was then removed by drying at 80^{O}c.The properties of FE-SEM allow for new approaches to life science studies to emerge, based on high-quality, low-voltage images with negligible electric charge of the samples, producing sharper images with less electrostatic distortion with a spatial resolution of 1.5 nm. 3 to 6 times better than traditional SEM. Low penetration is investigated for low kinetic energy electron sensors closest to the immediate material surface, as well as examination of smaller contamination areas at electron accelerating voltages compatible with energy dispersive X-ray spectroscopy[76],[77].

2.4.4 Transmission Electron Microscopy (TEM)

TEM is a technology developed to obtain far higher magnification and thus details of a specimen than ordinary optical microscopes. TEM generates a wealth of material information, including size distribution. Morphology, crystal structure, and TEM can be employed in a variety of applications, including research, nanotechnology science, and education. The TEM is based on the premise that when electrons are imposed on the surface of the specimen nanoparticles, they can scatter or backscatter elastically, resulting in a variety of interactions. ,The TEM can be used in various application such as research, science of nanotechnology and education.The TEM produces . 2D images with high resolution capacity[78],[79].

2.4.5 Band Gap Energy Measurements

A semiconductor is a substance that has poor electrical conductivity at ambient temperature but increases its conductivity when energy is applied to it. The solid material is made up of an infinite number of atoms and has an endless number of energy levels. Due to the close spacing of these energy levels, they form bands rather than distinct energy states. This is the primary distinction between a solid material and a single molecule with a finite number of atoms and discrete energy levels. The valence band is the highest energy band that is filled with electrons, The conduction band is the next higher band that is vacant.,The energy difference between these bands is known as the band gap, Eg [80].A Varian Cary 100 Scan UV−visible spectrophotometer system equipped with a lab sphere diffuse reflectance accessory was used to obtain the reflectance spectra,the bandgap was obtained for binary nanocomposites ZnO-CdS and ZnO-CdS/pd nano-composites powder[81].

2.4.6 Thermogravimetric Analysis (TGA)

TGA is an effective method for assessing the thermal stability of materials, particularly polymers. With this technique, a specimen's weight variations are monitored as its temperature rises. GA can be used to measure the moisture and volatile contents of a sample. The apparatus essentially consists of a programmable furnace to regulate the sample's heating up and a very sensitive scale to monitor weight change.A contemporary device that can compute the percentage or fraction of weight reduction shown in figures (2–9) and is typically computer-equipped. Determining the organic and inorganic makeup of samples as well as the material's distinctive decomposition pattern is a popular application of TGA[82].

Fig 2.8: Thermal gravimetric analysis

2.5 Applications of Prepared Nanomaterials

2.5.1 Determination of Maximum Wavelength (λ max) and calibration curve of Brilliant green dye

A standard solution of brilliant green color at 1000 ppm was prepared by dissolving a specified weight (0.1 g) of solid green brilliant dye in 1000 mL of distilled water, stirring to complete dissolution, and then completing to 1000 mL . The wavelength of the bright green dye in the range (200-800) nm was taken using a quartz cuvette. The maximum wavelength of the dye Solution was determined from its highest absorption in the UV-Visible spectrum, which was found at the wavelength (λmax= 630nm), the structure of the brilliant green dye is shown in Fig **2.10**. To construct the calibration curve for the brilliant green dye, a series of solutions were prepared by successive dilution of the dye standard solution with concentrations in the range (25-100)ppm. The absorption of this solution was recorded(λmax=630nm)

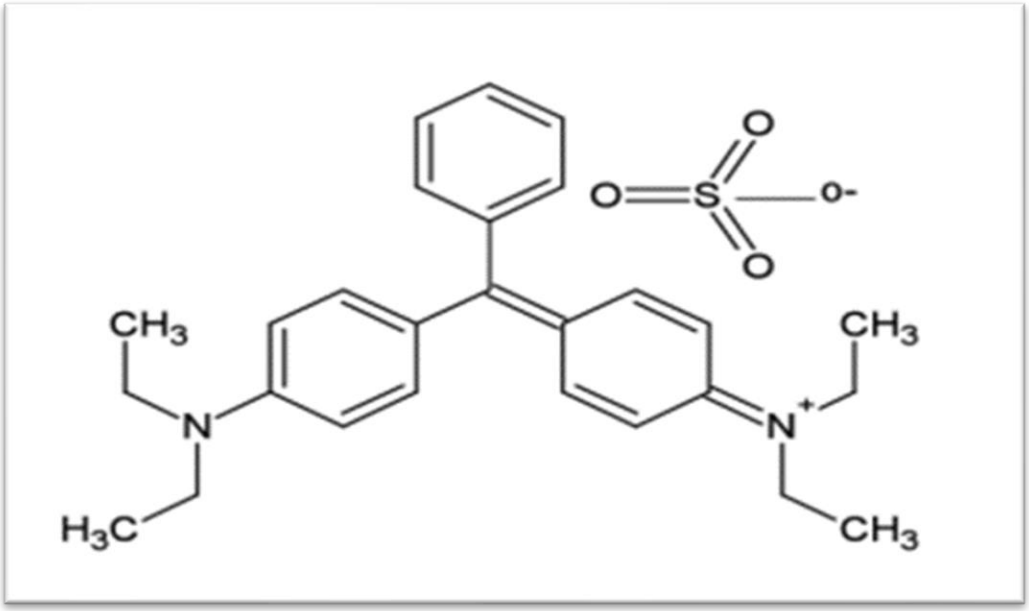

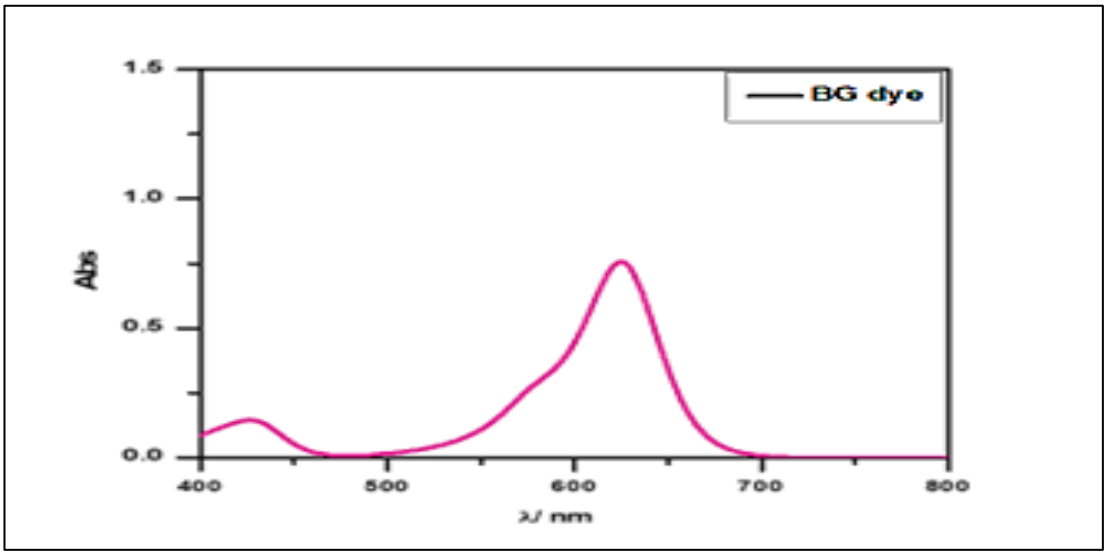

Fig 2.10: Structure of Brilliant green dye and Calibration Curve of Brilliant green Dye Solution [86]

2.6 Photo Catalysis Experiment

The photo catalytic activity of the ZnO-CdS\Pd nanoparticles catalyst was evaluated by the degradation of Brilliant Green (BG) dye. All experiments were carried out in a photo- reaction vessel, the beaker was put under UV light and the distance between the light source and the surface of the solution controlled by using UVA-meter. Experimental tests were performed, and 0.4 g ZnO-CdS\Pd photo catalyst was added to a 200 mL solution of BG dye. The mixture was maintained in the dark for 10 min under stirring to reach adsorption equilibrium, and was then irradiated at different time intervals for 1 hr. And speared by centrifugation at 3500 tr/min for 10 min .The concentration of BG dye was determined by measuring the absorption at its maximum absorbance wavelength of MG dye =630 nm, by using a UV-Vis spectrophotometer(UV mini-1240 Shimadzu, Japan) with a3 cm path length spectrometric quartz cell, and then calculated from calibration curve .The Effect of various operational parameters such as amount of catalyst (0.1-0.6 g/L) ,concentration

of dye(50-100mg/L) , light intensity (2.3-1.3) on the photo degradation efficiency was studied.

The percentage removal of photo catalytic degradation of BG dye and apparent first order rate constant were calculated using the following relationship :

$$\text{PDE}(\%) = \frac{C_0 - C_e}{C_0} \times 100$$

Where C_0 and C_e are the initial and final concentrations (mg/L) of dye in solution, respectively.

Fig 2.12: Real image for the experimental photo reaction

2.7 Removal of Pollutants (Dyes) by Using ZnO-CdS\Pd nanoparticles

A laboratory sample of 100mL of dye pollutants containing (Brilliant Green(BG) , Congo Red (CR), Methyl Violet (MV), Crystal Violet (CV), Methylene Blue (MB) , Brilliant Blue (BB) , Direct Yellow (DY) , and Reactive blue (RB) with a riffle concentration Was used in this study, then added to a conical flask (Erlenmeyer) in the presence of 0.4g Of prepared ZnO-CdS\Pd nanoparticles, After

that the mixture was put in Shaker water bath for 1hr, after that the supernatant was separated by centrifuge and measured the remaining concentration by using a UV-Visible spectrophotometer .

2.8 Reusability and stability of the pd doped ZnO-CdS nanocomposites

The recyclability of Pd doped ZnO-CdS nanocomposites was examined for Six consecutive cyclic runs . After each cycle, the nanocomposites were removed from the degraded BG dye solution and separated through ultra-centrifugation. This nanocomposite catalyst was washed thoroughly with distilled water followed by drying at 60 °C and then transferred to a fresh BG solution. It can be seen that the photocatalytic activity of the Pd doped ZnO - CdS nanocomposites decreased slightly to 2.2 % after four successive cycles due to the adsorption of intermediate products on the photocatalyst active sites .

3.0 Results & Discussion

3.1 Characterization of the prepared nanocomposites

3.1.1 X-ray diffraction (XRD)

The X-ray diffraction technique was used to study the crystallinity of the synthesized ZnO-CdS nanocomposite as a catalyst, and measure the particles size of the synthesized catalyst . XRD analyses of the prepared nanocomposite were carried out using XRD6000, Shimadzu, Japan. The measuring parameters were set with 45 Cu Ka radiation 0-1.54056 A) at 40kV, 30mA with a rate of 5deg/min and ran in the 28 range (3-90). The average crystallite sizes of the synthesized ZnO-CdS nanocomposite were measured according to the Scherer equation. The calculated value is are in the range of 25–30 nm .The X-Ray diffraction patterns of zinc oxide and ZnO-CdS nanocomposite at 500°C are observed in Table 3-1 and Fig. 3-1, The diffraction pattern Nine peaks appear at 31.7°, 34.4°, 36.2°, 47.5°, 56.5°,62.82°, 66.4°,67.9°and 69.10, which correspond to the (100), (002), (101), (102), (110), (103), (200), (112) and (201),reflection planes, in the same order . Which is represented by the pure ZnO as a hexagonal wurtzite phase (JCPDS-00-036-1451). The CdS crystal structure also exactly matches with the JCPDS card no.89-2944 and it also possesses better crystalline structure and pure phase with highly crystalline production due to sharp and intense peaks[81],[83]The main semiconductor device peaks of ZnO and CdS appear in the XRD of binary nanocomposites of ZnO-CdS (Figure 3-1). Additionally, in binary nanocomposites, the CdS peaks aren't sufficiently very strong. The cause is the crystalline ZnO NPs phase with a fourth concentration of CdS set thereby and CdS also has less crystallinity than ZnONP.

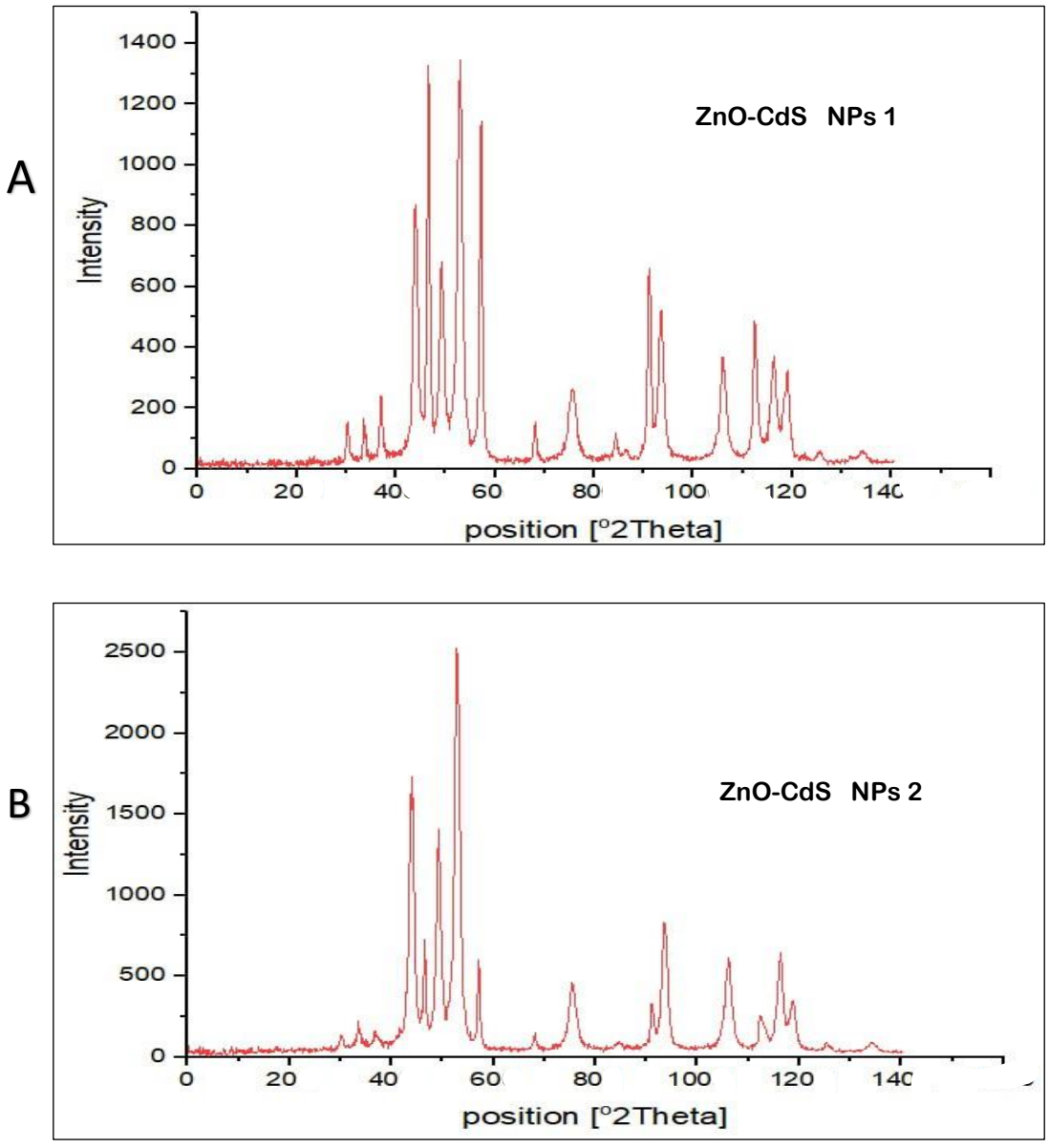

Fig 3.1: XRD Diffraction Patterns of (a) ZnO-CdS NPs 1 and (b) ZnO-CdS NPs 2

Furthermore, no impure peaks appear in the ZnO -CdS nanocrystalline plane which confirms the formation of ZnO -CdS binary composites. In Pd doped ZnO -CdS nanocomposite, the diffraction peaks only reflect the binary crystalline structures of ZnO and CdS. However, no characteristic peak of Pd is found which may be because of low content and weak intensity of Pd. Further, an increase in Pd amount on ZnO -CdS binary structure, intensifies the diffraction peaks gradually which indicates that the high crystallinity photocatalytic activity of Pd doped ZnO -CdS nanocomposites for the degradation of BG under light irradiation nanocomposites only doping of

transition metal (Pd). This type of crystalline behavior of ZnO -CdS binary composites may be responsible for better photocatalytic catalytic activity[84] .

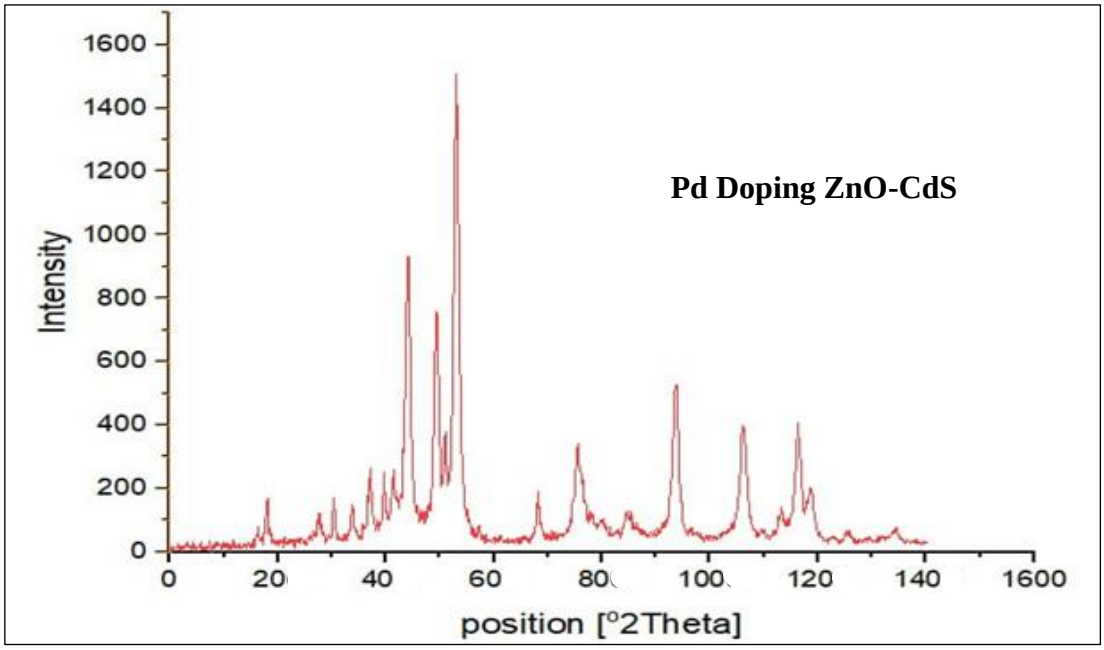

Fig 3.2: XRD Diffraction Patterns of Pd Doping ZnO-CdS

3.1.2 FE- SEM of ZnO -CdS and Pd /ZnO-CdS Nanocomposite

FE-SEM images of different structures are displayed in Figs.(3-3)and (3- 4). It was conducted to reveal the morphological characteristics of different samples. The FE-SEM photograph of the ZnO -CdS which was prepared by the hydrothermal method and calcinated at 500k for 1h is shown in Figs.(3-3), additional metal doping (Pd) on ZnO -CdS nanoparticles surface has been also shown in Fig.(3.4) showed up as spherical pallets with a very even surface. However, some agglomerated surface areas were also noted, particularly in pallets smaller than 200 nm. Platforms were widely dispersed and the surface of the ZnO-CdS binary nanocomposites (Fig3.3) was rough. It was watched using a stretcher with a size of 200 nm. a Pd-doped ZnO-CdS nanocomposite that exposed a new column of spherical nanostructures. The palladium ion in the ZnO-CdS lattice was depicted in the figure, and this conformation is adjustable . The ZnO-CdS overlaid dopant Pd showed uniform size and good porosity,

making it a distinctive and ideal surface for absorbing brilliant green dye, as seen by comparing Fig 3.3 . The uniform size and great porosity of the ZnO-CdS overlaid dopant Pd, which made it a distinctive and ideal surface for absorbing brilliant green dye, caught our attention. Fig (3.4) showed how the surface of the initial binary nanocomposite was altered by the addition of palladium, showing nanoparticles as an unclear agglomerated surface. Due to the additional Pd dopant in ZnO-CdS binary nanocomposites, the uneven agglomerated surface displayed a higher particle size.

So a small reduction of the size grain is observed when doping Pd on to ZnO - CdS and the surface grossness remains same and seen to be nearly symmetrical. pd metal was found to be overlapped with ZnO-CdS nanocomposites which exhibit cubic like morphology and particle size[85],[27],[86].

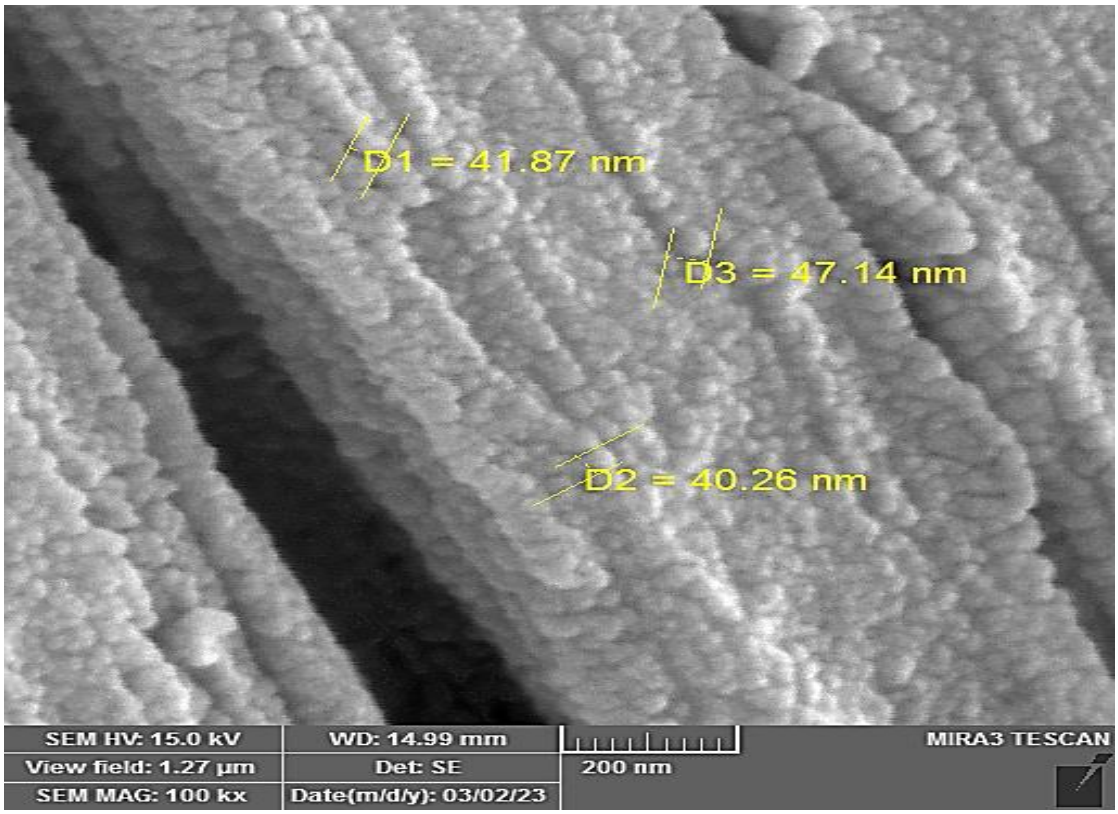

Fig (3-3) The FE-SEM photograph of the ZnO -CdS NP2

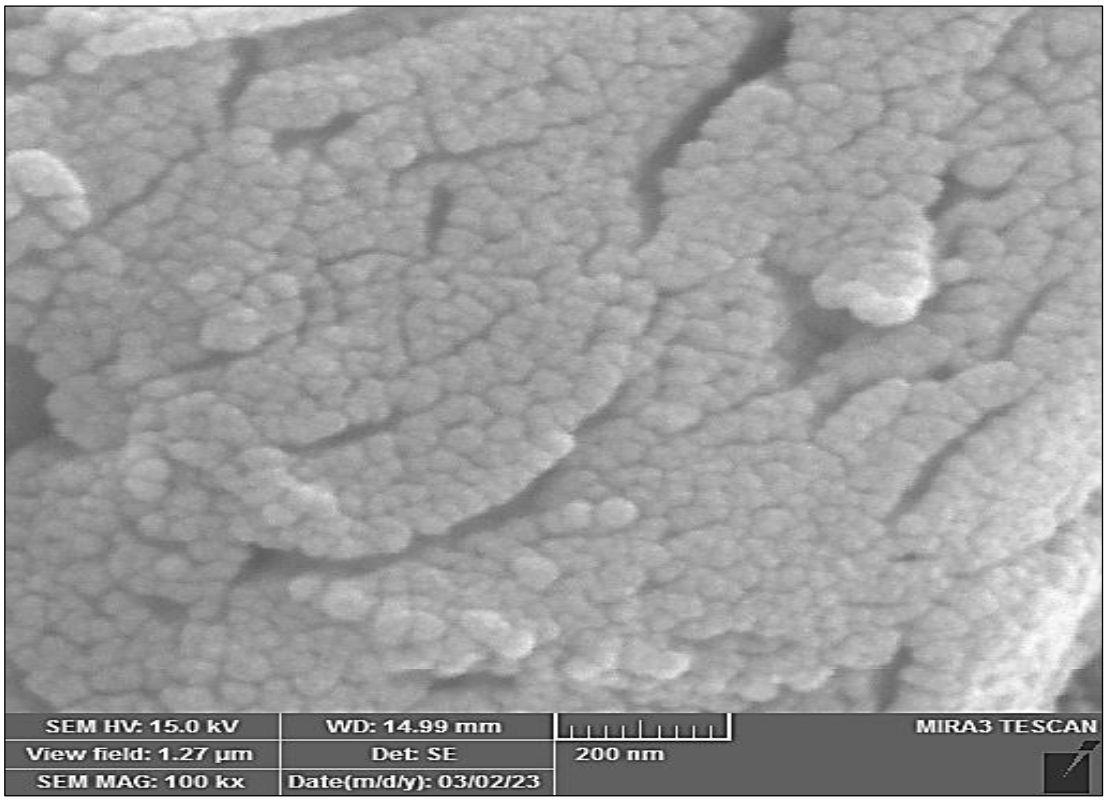

Fig 3.4 The FE-SEM photograph of the Pd Doping ZnO -CdS nanocomposite

3.1.3 The transmission electron microscopy TEM of ZnO -CdS and Pd /ZnO-CdS Nanocomposite

TEM images were obtained to determine the particle size, morphology and crystal structure of ZnO -CdS and Pd /ZnO-CdS nanocomposites. Fig (3.5)(a) and (b) show that the average size of ZnO -CdS and Pd /ZnO-CdS nanocomposites is approximately 200 nm. TEM images show the presence of CdS nanoparticles on the flakes of ZnO (Fig (3.5)(a) (a magnified image). A Magnified view shows the single crystalline nature of ZnO and CdS which is marked by with red colored circles. ZnO/CdS may be due to orientation disorder between the ZnO nanoparticles and the CdS nanoparticles.The surface particle structure of the Pd doped ZnO -CdS nanocomposite, which is present in a spherical stacked structure, is depicted in (Fig.

3.5 b). Additionally, ZnO, CdS, and Pd are packed together closely. The uniformly integrated Pd ion on the surface of the ZnO-CdS nanocomposites is shown as a dense, small spherical dot in(Fig 3.5 b).The uniformly dispersed, doped ZnO-CdS nanostructure had a size of 200 nm. Several research results have supported the optical effective mass approximation model, which suggests that the particle size is affected by the amount of doping present, and it decreases as the degree of doping increases. TEM images revealed the poor crystallinity of Pd-doped ZnO-CdS nanocomposites. Our findings demonstrated that the Pd ion was effectively deposited onto the ZnO-CdS surface and that the binary ZnO-CdS was successfully assembled[87],[85],[88].

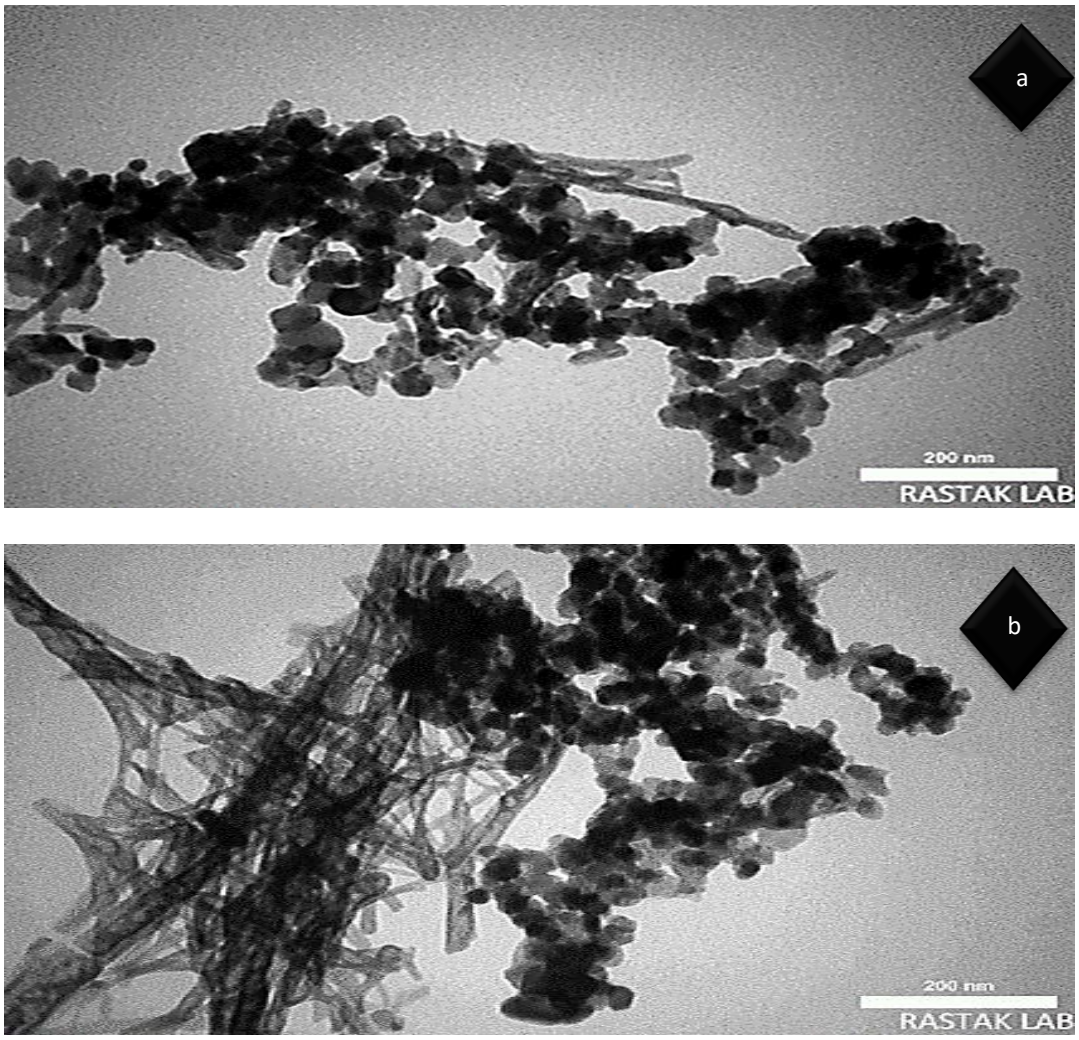

Fig 3.5: TEM (a) ZnO-CdS NPs ,(b) ZnO-CdS/pd nanocomposit

3.1.4 Thermo Gravimetric Analysis ZnO -CdS and Pd /ZnO-CdS Nanocomposite

The thermal stability of the ZnO -CdS and Pd /ZnO-CdS Nanocomposite was examined at the temperature range of 50–800°C with a heat in grate of 10°C/min, under nitrogen flushing at 200 mL/min using Boyuan DTU-2C thermogravimetric analyzer. As the temperature increased, a graph of weight loss (%) versus temperature was plotted. ZnO -CdS and Pd /ZnO-CdS Nanocomposite were subjected to TGA to determine the thermal stability and decomposition characteristics[30].

A thermogravimetric analysis was conducted on the sample obtained from the binary composite and the nanocomposite after palladium doping (Fig. 5). The analysis revealed no significant weight loss, indicating the excellent thermal stability of the prepared composite[89],[90]

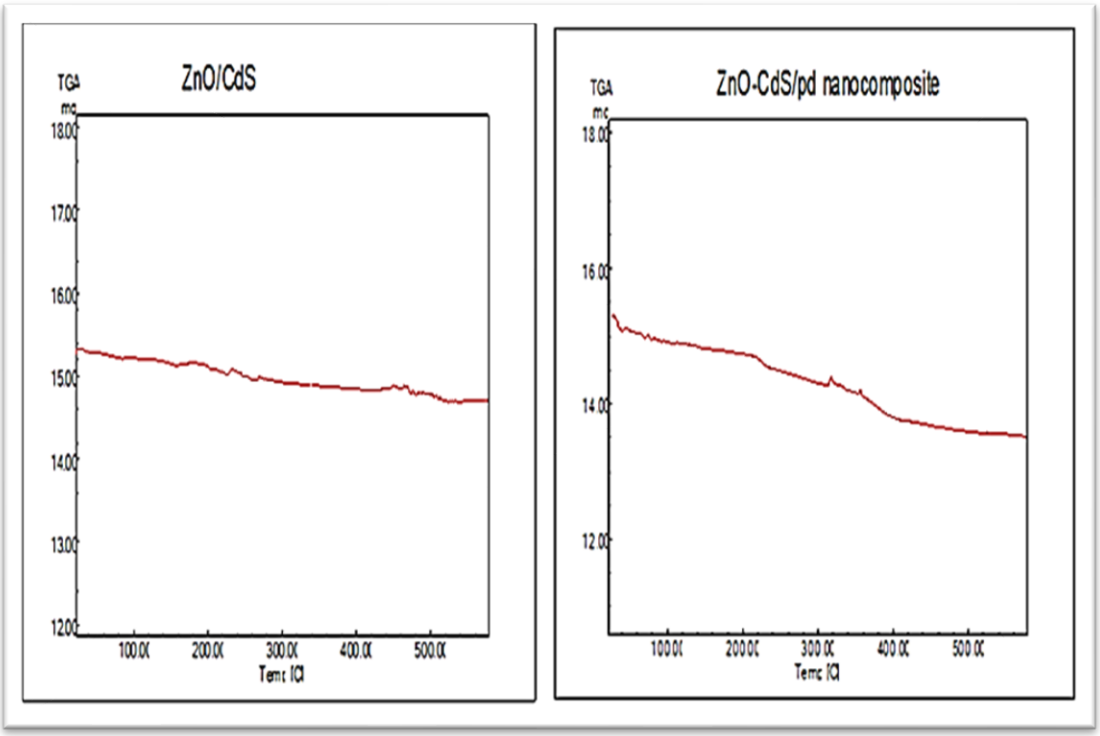

Fig 3.6 TGA analysis images of ZnO-Cds CdS , a) ZnO- CdS/Pd nanocomposites

3.1.5 UV-Vis Spectroscopy of of ZnO -CdS and Pd /ZnO-CdS Nanocomposite

Studies of the optical characteristics of these particles employing UV-Vis Spectroscopy in the range of wavelengths 300-700 nm have determined the size of the energy band gap of created nanocomposites.Based on the sample's absorption spectrum, the band gap energy was determined using the formula below:

$$Ebg = 1240/\lambda g$$

Where, Ebg is The band gap energy of the photocatalytic, λg is the wavelength in nm usedfor the absorption edge. Also the band gap of nanocomposites can be calculated by Tauc's plot which is expressed as follows:

$$(\alpha h\nu)^{1/n} = Cx\ (h\nu - Ebg)$$

Where α is the absorption coefficient, h is Planck's constant, andν is frequency (ν = c/λ, c light speed, λ is the wavelength). n = ½, 2 for direct and indirect.

Semiconductor materials' band gaps significantly affect their electrical and optical characteristics, hence it is important to research variations in band gaps for the better understanding of the relevant aspects of this class of materials. The optical characteristics of nanoparticles can be discovered using absorption spectroscopy. The UV and visible range absorption spectra of ZnO-CdS and ZnO-CdS/pd nanocomposite at various thermal treatment temperatures are presented. All of the spectra had absorption edges between 370 and 390 nm, which is consistent with the intrinsic band gap absorption of zinc oxide caused by electron transitions as a value for conduction bands (O 2 p ZnO 3d).Fig (3.7) shows how experimental findings suggest that ZnO NPs have a wider band gap than larger spherical crystals. This can be explained by the nanoscale properties of materials.

This improvement in the optical absorption of ZnO-CdS is caused by the increase of defect sites on the catalyst structure which can inhibit the recombination of the charge carriers and improve the photocatalytic activity of ZnO-CdSy. The band gap of ZnO-CdS binary nanocomposites is smaller than that of the parent ZnO, due to the CdS cover with ZnO. When Pd is doped on the ZnO-CdS matrix, decreasing the band gap (2.32 eV) reveals that the Pd ion has changed the band structure of ZnO-CdS binary nanocomposite.According to the results, the band gap slowly decreases with the increase of the Pd doping ZnO-CdS anda small change was observed[91-94].

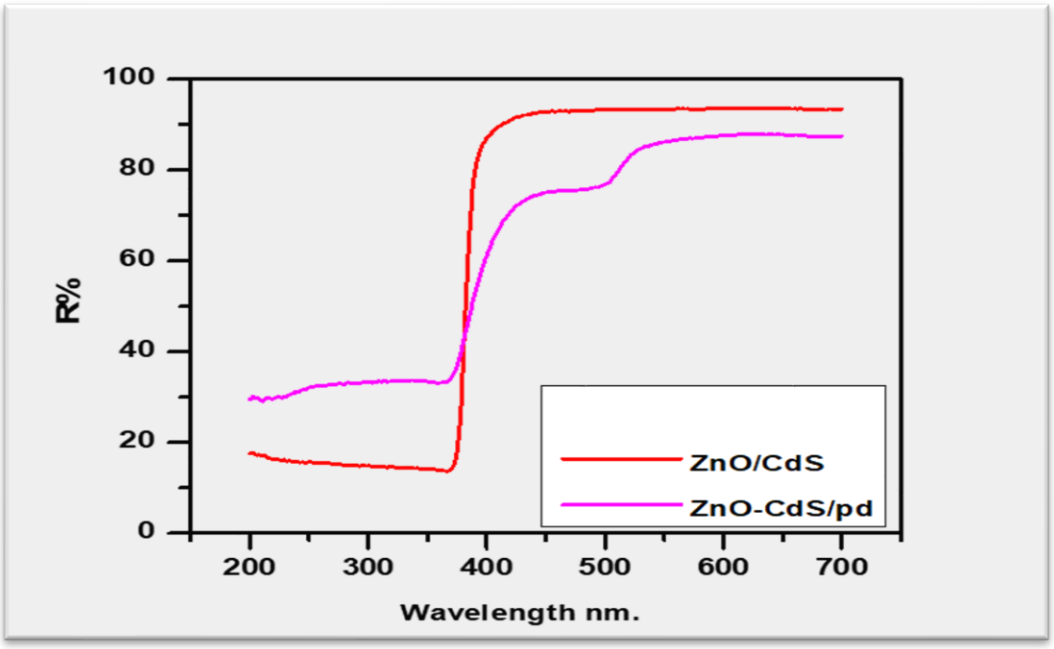

Fig3.7 : Diffuse Spectra ZnO -CdS and Pd /ZnO-CdS Nanocomposite

3.2 Selectivity of the Best Photo Catalyst Surface

The Ag and Pd content play an important role in increasing the optical efficiency and preventing electron-hole pair recombination. It is known that metal nanoparticles deposited on the surface of ZnO-CdS binary nanocomposites act as effective traps for photogenerated electrons due to the formation of a Schottky barrier

upon contact with metallic semiconductors. These electrons improve the rate of oxygen reduction and prevent electron-hole recombination[95] .

When Pd and Ag nanoparticles come into contact under illumination, photogenerated electrons are distributed between both types of particles, resulting in electron transfer from excited ZnO-CdS binary nanocomposites to Ag and ZnO-CdS binary nanocomposites to Pd until the two systems reach equilibrium. The electron accumulation of the Ag and Pd particles raises the Fermi level to a greater negative potential, causing the compound's Fermi level to shift closer to the conduction band of the composites[96].

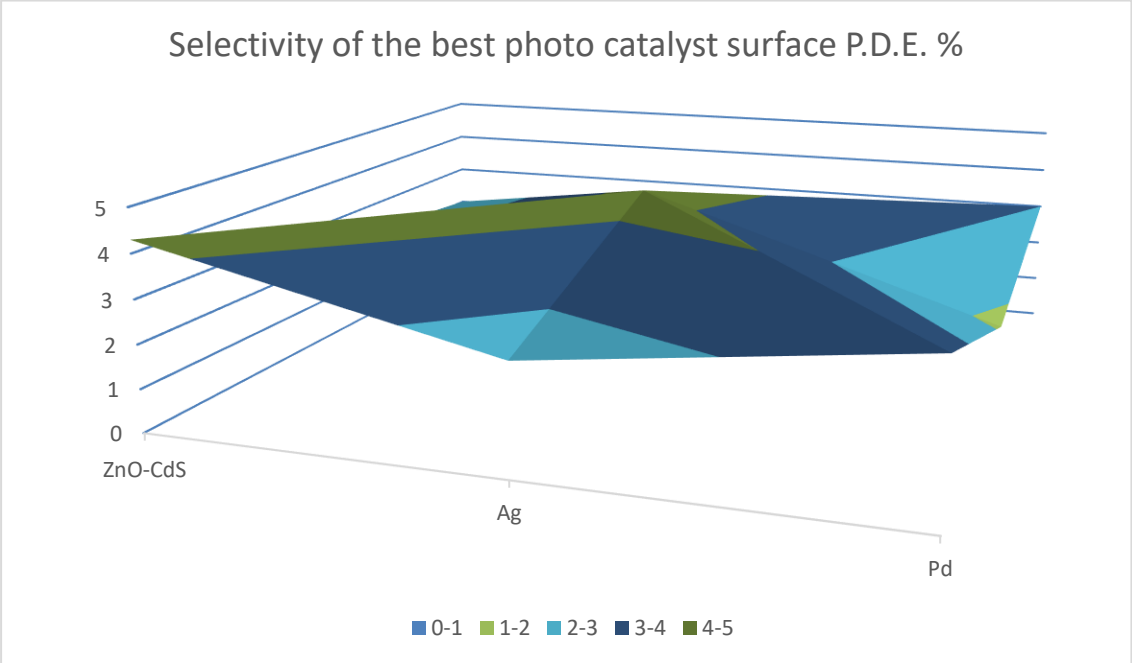

Fig (3-8): Selectivity of the best photo catalyst surface P.D.E. % with type of Nano catalyst

Fig.3.7shows a significant and noticeable increase in the photocatalytic degradation efficiency of pd Doping on ZnO-CdS In contrast, a decrease in the photolysis efficiency of the remaining types of Nanocatalysts. for the dye's photodegradation reaction, the dye solution was employed at a concentration of (50 ppm) with UV light irradiation, but without the use of the Nano catalyst surface (the catalyst), which

indicates a minor drop in the dye's C/C₀ value .When comparing the stages of the reactions in the dark and under the influence of ultraviolet light, which were illustrated in the previous figures, where the change was in the dye's concentration, the photolysis of the BG dye with the individual metal Pd , Ag with the binary and nanocomposites ZnO-CdS respectively[31], But, in the dark, it is also low because of the dye's Adsorption on the surface of the catalysts, which is dependent on surface area, as well as a decline in dye concentration in the presence of the surface. The catalyst's selectivity It is determined by the adsorption of reactants on the surface of the catalyst. When the Pd g loading is greater than that of type Ag, however, the active sites on the ZnO-CdS surface that are available for light absorbers and electron donors are covered with extra Pd particles. Furthermore, some Pd particles have previously been shown to behave as recombination foci for photogenerated electrons and holes with Pd loading[97].

Finally, using palladium in the decomposition process led to excellent results with a removal rate of more than 80%. As a result, the research methodology was settled on determining the overlay after subjecting both catalysts to the same optimum conditions with the same concentration of the dye BG. As a catalyst for BG Dye, it achieves its best.

3.3 Application of Prepared Nanocomposites

3.3.1 Photo Catalysis Experiment

3.3.1.1 Effect concentration of Brilliant green (BG) dye

To evaluate the use of a solution-grown Pd-doped ZnO -CdS nanocomposite as a photodegradation catalyst for the textile pollutant Brilliant green dye. The initial concentration of dye solution is crucial in determining the rate of dye breakdown. We studied their photocatalytic breakdown kinetics at room temperature

in the presence of UVA light at wavelengths ranging from 370 to 390 nm[98]. Because the generation of valence band holes on the surface of the photocatalyst required for reacting with dye molecules does not increase as the intensity of light and the amount of catalyst remain constant, a decrease in photocatalytic Degradation Efficiency was observed, most likely due to the blockage of hydronium cation adsorption at surface active sites, resulting in a reduced ability to produce hydrogen[99].

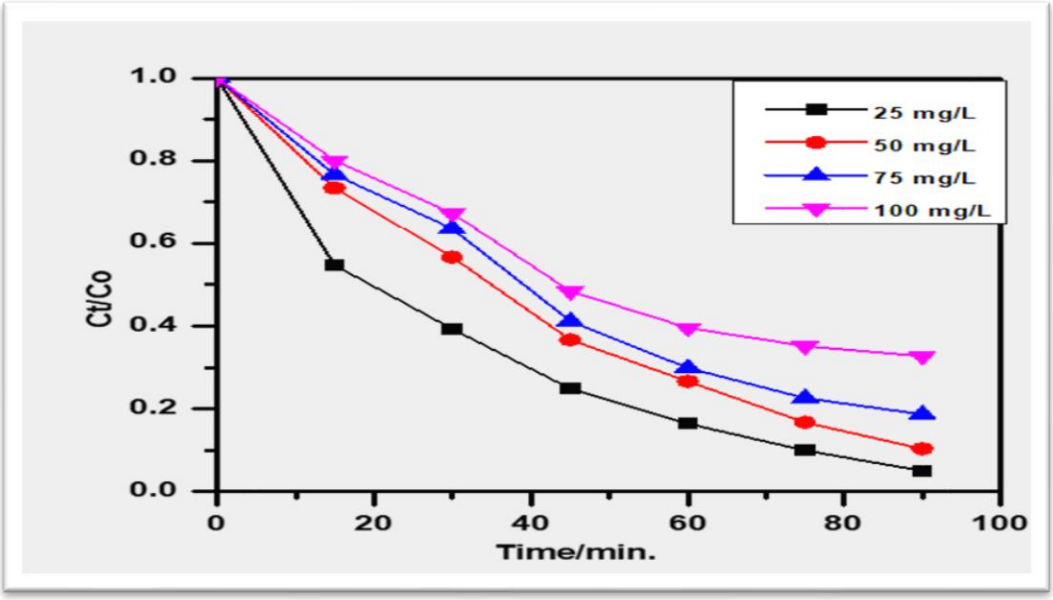

Fig3.9: Effect Photocatalytic degradation by nanocomposite at different concentration of BG dye

Concentrations ranged from 25 to 100 ppm. The optimum P.D.E. dye solution with an 86% concentration is 50 ppm. In terms of dye concentrations used and their dissociation rates with the catalyst Nano surface effective.Furthermore, at high dye concentrations, excessive dye adsorption may cover the active sites on the ZnO-CdS-Pd surface, resulting in a decrease in hydroxyl radicals in dye hydrolysis and a slower dye breakdown rate.[100]

As shown in Fig(3-10), the dye photocatalytic degradation efficiency (PDE%) rises with decreasing dye concentration, increasing from (95.76% to 67.98%).

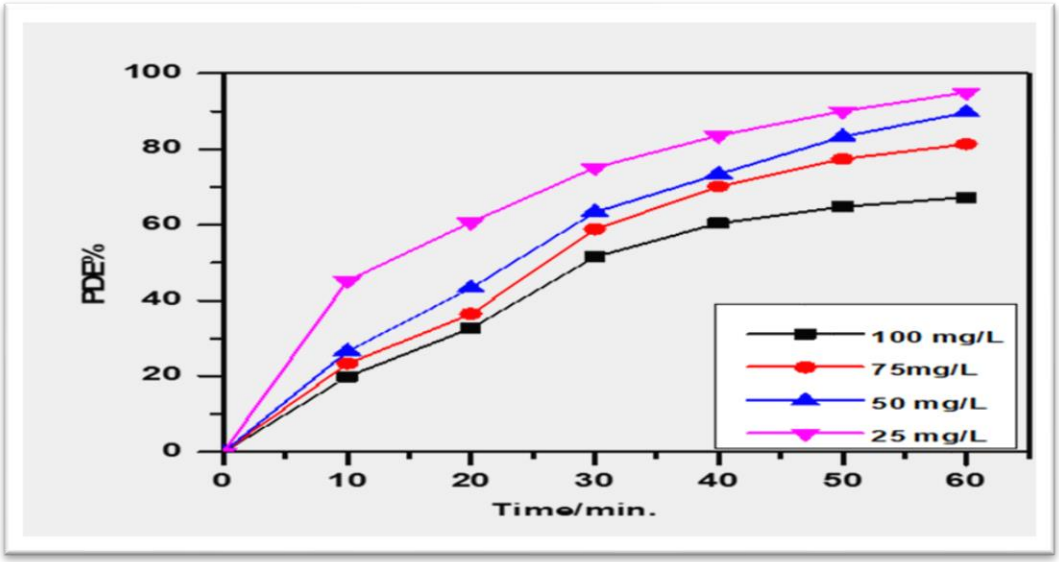

Fig3.10: Effect concentration of BG dye on the PDE%.

3.3.1.2 Effect of mass nanocomposite

The influence of the photo catalyst concentration (25 - 100 gL-1) on the photo catalytic degradation of ZnO -CdS\Pd NPs was investigated at an initial BG dye distance between the light source and the surface of ZnO -CdS\Pd NPs by using UVA-meter (Dr. Holne/Germany)for 1hr, after that the supernatant was separated by centrifugation and measured the remaining concentration measured by using a UV-Visible spectrophotometer at a chosen wavelength of 630 nm and found when time increase the absorption decrease and gave higher percentage removal[101].

Under the effect of ultraviolet radiation, the decomposition rate was investigated using various catalyst weights ranging from (0.1- 0.6 g). The catalyst surface acts to minimize activation energy, allowing more molecules to have activation energy and thereby increasing the reaction rate. When using catalysts, small amounts are used. Increasing the amount of catalyst used in the reaction after a certain point

does not result in an increase in reaction rates.The photocatalytic degradation of the BG dye after extracting it at its greatest concentration (50 ppm) utilizing surface ZnO-CdS-Pd NPs of varied weights while subjected to UV radiation for 60 minutes. The maximum value of photocatalytic degradation efficiency (86.33) was obtained when weighing (0.4 g), while the lowest value of photocatalytic degradation efficiency (55.1%) was obtained when weighing (0.1 g). The increase in the weight of the catalyst surface increased the number of active sites on the catalyst surface. which is what caused the values of P.D.E. to increase and decrease. A higher than necessary concentration of the catalyst will result in more suspended particles in the dye solution, which will subsequently subsidize the suspension and reduce penetration, The utmost optimum conditions are BG dye concentration of 50 mg/L , light intensity (2.7 mW/cm2, and solution pH 6.8) .When the mass of the nanocomposite increased, the rate of degradation rose because increase number of active sites. In the region between 0.1g and 0.6 g , there appear an approximately plateau curve which indicates the numbers of active sites have an equilibrium between the numbers of photon induced and absorbed by the catalyst and a particle of dye adsorbed represents the percent degradation of dye against the several quantities of nanocomposite [102].This shows that the percent degradation of modified catalysts rise with increase in amount of catalyst from 0.1 gL^{-1} to 0.6 gL^{-1} and above this limit there is not much change.

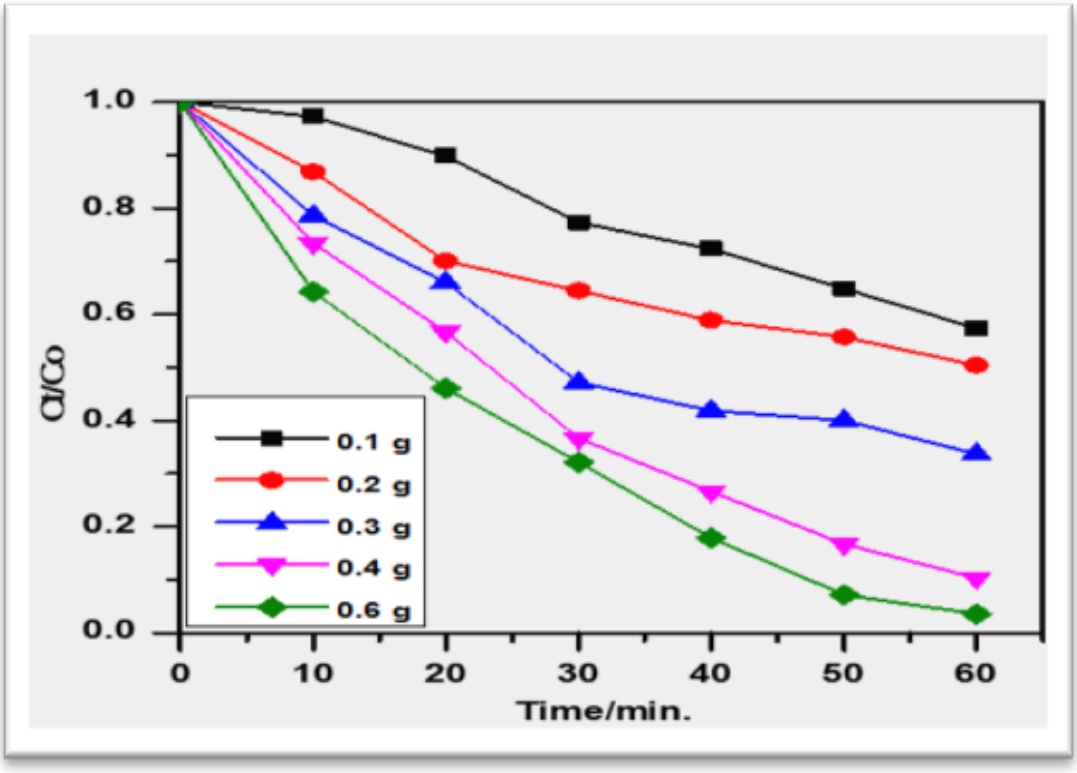

Fig 3.11: Photo catalytic degradation of BG dye at different weight of nanocomposite

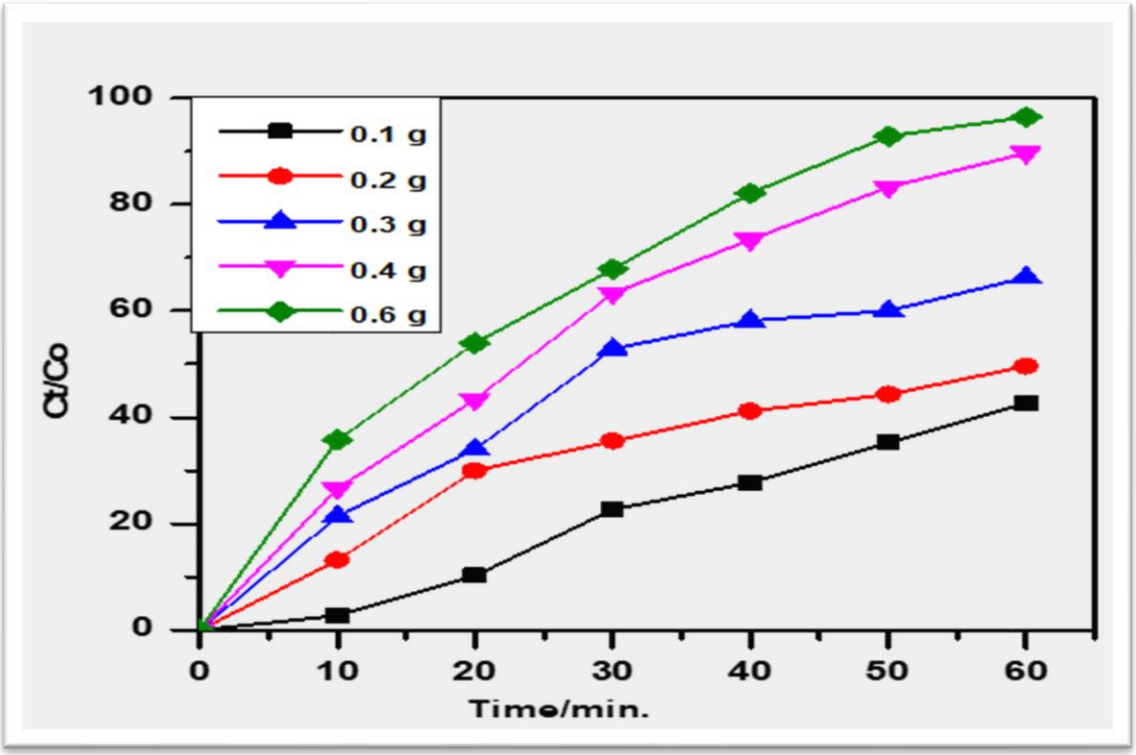

Fig3.12: PDE% BG at several weight of nanocomposite

3.3.1.3 Light Intensity Effect on Photodegradation of the Dye

The extent of light absorption by the semiconductor catalyst at a given wavelength is determined by light intensity. The rate of photocatalysis initiation, electron-hole (e-/h+) formation, and formation in the photochemical reaction are all substantially dependent on light intensity. The overall pollutant conversion and degradation efficiency are invariably determined by the distribution of light intensity within the reactor. As a result, the dependence of pollutant degradation rate on light intensity has been explored in multiple organic pollutant studies.. The photocatalytic degradation efficiency rate increases with the UV light's intensity as more radiation falls on the catalyst and, therefore, more hydroxide radicals [103, 104]They are produced, resulting in a high rate of photocatalytic degradation efficiency. It has been shown in Fig. 3.13.

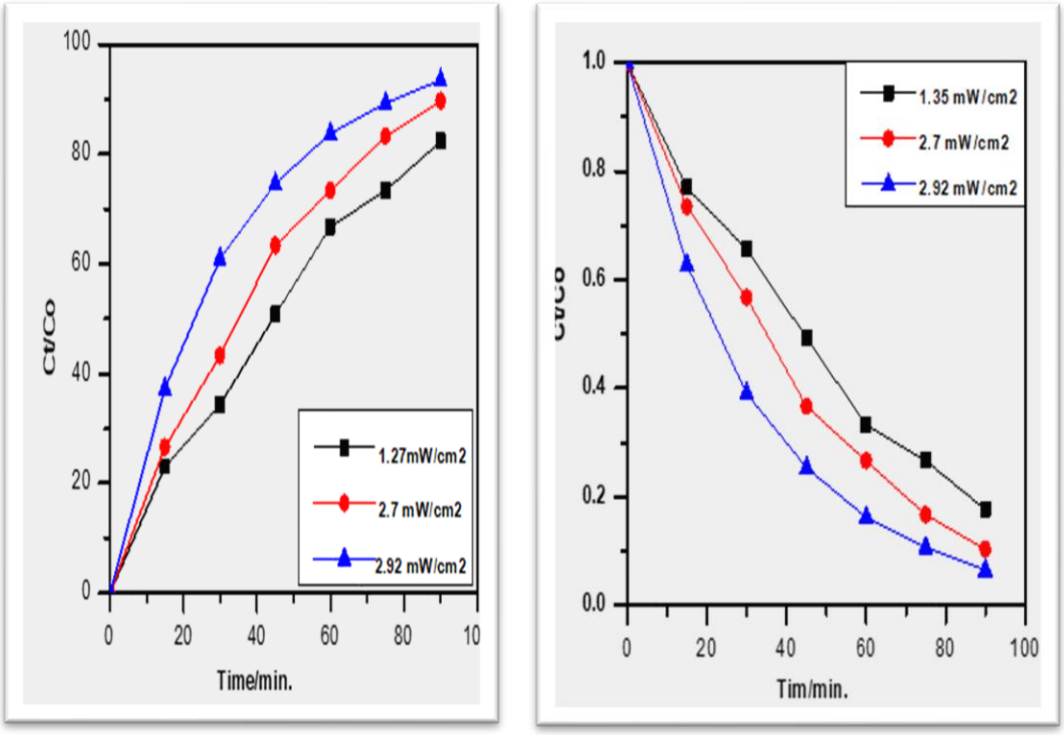

Fig 3.13: Effect of Light Intensity on P.D.E. % of Brilliant Green Dye

At low light intensity (2.3-1.3mW.cm-2), the rate will increase linearly with increasing light intensity (first-order), while at intermediate light intensity (1.27 mW.cm-2) the rate will depend on the square root of light intensity, In high light, the rate independent of light intensity. Low intensity reactions involving electron-hole formation (ē) are predominant and electron-hole recombination (ē) are non-significant[9]. The higher the incident light intensity in the lower light intensity range, the larger the rise in the absorption potential between photons and active sites on the ZnO-CdS-Pd surface. When the light intensity increases, however, the separation of electrons and holes competes with recombination, leading the reaction rate to decrease[105].

3.4 Removal of Pollutants (Dyes) by Using ZnO-CdS\Pd nanoparticles

In this experiment, 100 mL of real sample (a mixture of dye pollutants consisting of brilliant green dye BG, Congo red (CR), methyl violet (MV), crystal violet (CV), methylene blue (MB), brilliant blue (BB), and other toxic textile dye) with a refry concentration were used, then beakers in the presence of 0.4 $gL^{-1}$of ZnO-CdS-Pd nanoparticles, were added and after that the mixture the beaker was put under the ultraviolet [106],[107] show in Fig 3.14 . and found when time increase the absorption decrease and gave a higher percentage of removal show in Fig 3.15, presents the results, which indicate that photocatalytic degradation of at least 80% was achieved using0.4goftheZnO-CdS/Nanocomposite.

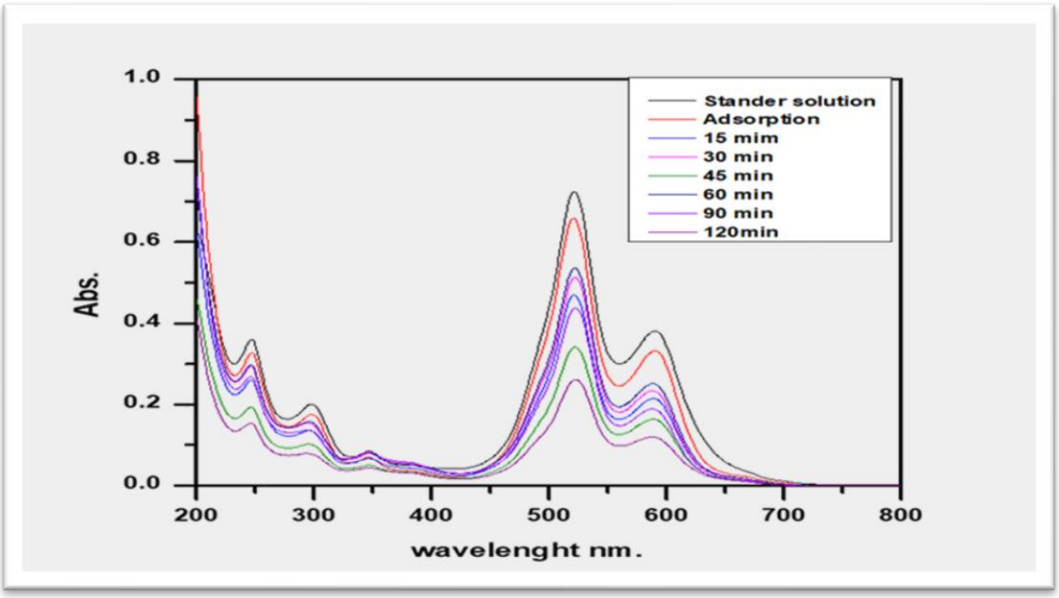

Fig 3.14: Removing the mixture of pollutants under test conditions

Fig 3.15 Real Photo of real sample mixture of dye pollutants

2.5 Reusability and stability of the pd doped ZnO-CdS nanocomposites

The stability and reusability of target materials are another important standard for practical application. After adsorption experiments, adsorbents can be separated by simple centrifugation due to their insoluble properties in water[108]. As shown in

Fig3.16 in the four cyclic BG tests, the ZnO -CdS\Pd nanocomposites exhibited an excellent stability with an average BG removal efficiency, and no evident change has taken place for the photocatalytic activity, which indicated good photocatalytic stability of the ZnO -CdS\Pd nanocomposites[85] . The evaluation of photocatalyst photostability and durability under repeated photocatalytic cycles is critical for practical applications. The cyclability of pd-doped ZnO-CdS nanocomposites was investigated throughout four consecutive cyclic runs.After each cycle, the nanocomposites were isolated from the deteriorated BG dye solution by ultracentrifugation[109]. This nanocomposite catalyst was completely rinsed with distilled water, dried at 100 °C, and then transferred to a new BG solution. The photocatalytic activity of the pd doped ZnO-CdS nanocomposites was reduced marginally to 2.2. % after four successive cycles due to adsorption on photocatalyst active locations. The photocatalytic degradation of BG dye was found to be 86.6%, 85.9%, 84.9%, 83.6%, and 82.2% for the first, second, third, and fourth cycles, respectively. This shows that the Pd doped ZnO-CdS nanocomposites are stable and might be used in practical batch degradation. However, the produced Pd doped ZnO-CdS nanocomposites exhibit significant stability under light irradiation.

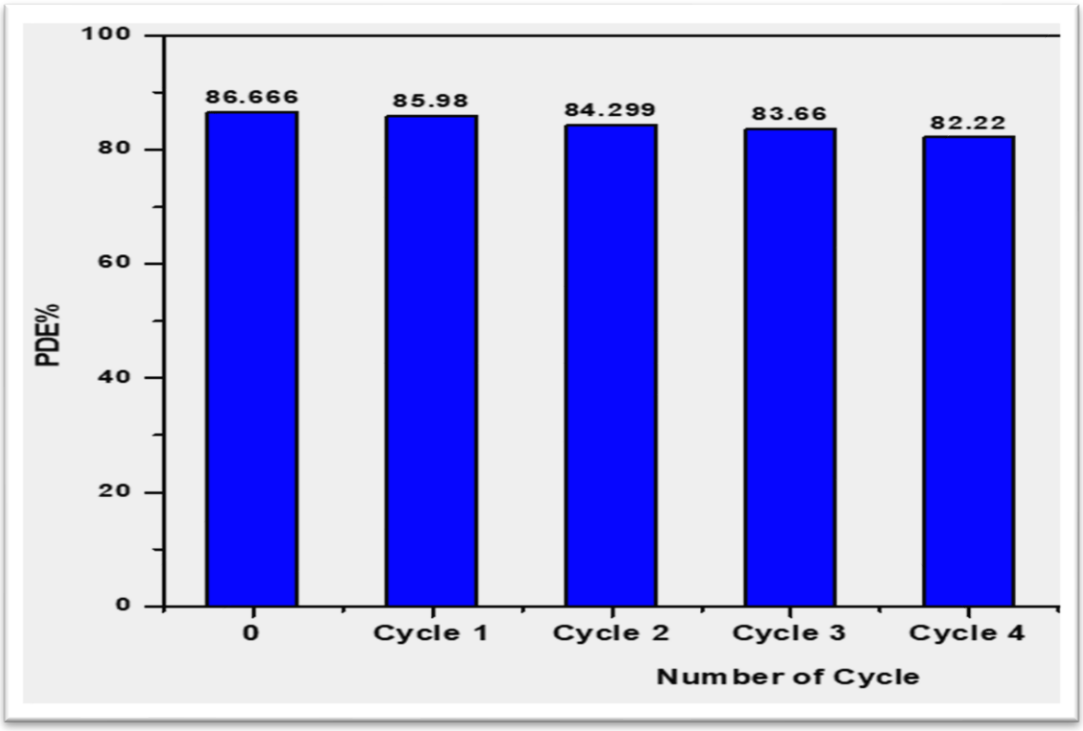

Fig3.16: Reusability and stability of the pd doped ZnO-CdS nanocomposites.

4.0Conclusions & Recommendations

4.1 Conclusions

1. The Hydrothermal method is usefully for synthesizing ZnO-CdS\Pd nanoparticles.

2. ZnO-CdS\Pd nanoparticles. shows good photocatalytic activity.

3. The Highest photocatalytic removal has been done in the presence of ZnO-CdS\Pd nanoparticles..

4- The concentration of BG dye at 50 mg/L gives the best Photocatalytic degradation capacity 86.66% .

5- Photocatalytic degradation efficiency (PDE%) increases as the dye concentration decreases from 86.66 % to26.9 % .%

6. Doping Pd on the surface of ZnO-CdS plays an important role of reduced the recombination process.

7. Photodegradation rate follows Pseudo first order kinetic, this attributed to the heterogeneous surface

8- Photocatalytic degradation increases with increasing mass of catalyst nanocomposite.

9- Nanocomposite surface appears to have good stability and can be reactivated after 4 cycle

.

4.2 Recommendations

1. Using other metal doping on semiconductors, such as M (Pt. Au, Mn) ZnO-CdS, for enhanced optical and photocatalytic properties.

2. synthesized new nanocomposite by using the green method.

3. Using the prepared surface as a model for antibacterial activity.

4. Using the prepared surface as a source of photoreduction for organic compound

5.Studying the effect of PH on the prepared surface.

6. Studying the effect of different time and different temperature on the prepared surface.